To study the thermal equilibrium in mass asymmetric nuclear reactions at intermediate energies

A dissertation submitted for the partial fulfillment of

requirement for

the award of the degree of

Master of Science

in Physics

Submitted by

Him Jyoti

Roll no. 301304003

Under the administrative guidance of

Dr. Manoj Kumar Sharma

School of Physics and Material Science
Thapar University
Patiala – 147004 (PUNJAB), INDIA

CERTIFICATE

I hereby declare that the report entitled "To study the thermal equilibrium in mass asymmetric nuclear reactions at intermediate energies" is an authentic record of my own work carried out for the partial fulfillment of the requirement for the award of the degree of M.Sc. (Masters of Science) at Thapar University, Patiala (Punjab), under the administrative guidance of Dr. Manoj Kumar Sharma, Professor, School of Physics and Materials Science. The matter presented in the dissertation has not been submitted in part or full for the award of any other degree.

Date: 14/07/2015

Him Jyoti

Him Jyoti

Roll No. 301304003

It is certified that the above statement made by the candidate is correct to the best of my knowledge and belief.

Administrative Supervisor

(Dr. Manoj Kumar Sharma)

Professor

School of Physics and Materials Science

Thapar University, Patiala

(Dr. Manoj Kumar Sharma)

Professor
Head
School of Physics and Materials Science
Thapar University, Patiala

(Dr. S. S. Bhatia)

Professor
Dean of Academic Affairs
Thapar University, Patiala

i

Acknowledgement

This work would not have come to fruition without the help, wittingly or unwittingly of a great many people too numerous to mention. This section provides a platform, to recognize and acknowledge those fortunate enough to spring to mind.

I would like to express my gratitude to my supervisor Dr. Suneel Kumar for the useful ideas, remarks, and engagement throughout the learning process of this master thesis. His varied perspectives have helped me to strengthen my work.

Furthermore, I would like to thank, Ms. Sangeeta, research scholar, School of physics and materials science, for introducing me to the topic, as well as for the support on the way. I would also like to thank all the research scholars working in the lab of theoretical nuclear physics at intermediate energies.

I would like to thank Ms. Loveleen Kaur Brar, Assistant Professor, and Dr. Kulvir Singh, Professor, School of Physics and Materials Science, for their valuable advice from time to time.

I am also grateful to the theoretical physics committee, which has given me a valuable feedback, which helped me immensely to improve my research work.

I would like to thank Dr. Manoj Kumar Sharma, Head, School of Physics and Materials Science for his support for providing me the necessary lab facilities.

Finally, I would like to express my heart-felt gratitude to my family, who has supported me both emotionally as well as financially. They have encouraged me enough, so as to complete this research work.

Date 14/07/2015

himjyoti

Him Jyoti

301304003

CONTENTS ---------- **Page No.**

List of Figures

List of tables

ABSTRACT

In the present study, the variation of temperature (of the hot central region formed in the heavy ion collisions) with the scaled impact parameter and rotational effect has been analyzed for various mass asymmetric nuclear reactions under the influence of soft equation of state using Isospin-dependent Quantum Molecular Dynamics (IQMD) model. The notable rotational effect is observed from the phase space dynamics and from the local density profile of the two asymmetric colliding nuclei. Afterwards the simulations have been carried out for the various reactions at the fixed value of incident energy and colliding geometry i.e. $\hat{b}$ for a fixed value of participant zone for each and every reaction. It has been observed that the $<T_{avg}>^{max}$ increases with increase in the mass asymmetry. A marked influence of rotational effect has also been observed on the $<T_{avg}>^{max}$ for the various mass asymmetric reactions.

CHAPTER 1

INTRODUCTION

The branch of nuclear physics deals with the properties of nuclear matter, and to explore the hidden concept of nuclear physics, it is very important for a nuclear physicist to know about the properties of nuclear matter. In heavy ion collisions, whenever two nuclear systems collide with each other, some energy is produced and this energy tends to elevate the temperature of the final composite system than that of the system's initial state. The simplest example of this process is the reaction of hydrogen nuclei in the "Sun". The proton-proton chain reaction in the sun gives rise to the temperature in the range of billionth of Kelvin. Hence the exploration of temperature is very important.

Fig. 1.1 is depicting the chronology of the universe. The story of existence of temperature started a long time ago when the Big Bang happened. In the very early stage, our universe was very hot. That state of universe had infinite energy density and temperature. Since 0 to 10^{-43}sec of big bang, due to so much high temperature, the four fundamental forces namely electromagnetic, gravitational, weak nuclear interactions and strong nuclear interactions were combined to known as one fundamental force. Thereafter between 10^{-43}sec and 10^{-46}sec, grand unification theory (GUT) came into picture. With increasing time, these forces parted their ways. After few microseconds (between 10^{-12}sec and 10^{-6}sec), due to high energy density and temperature quarks, antiquarks and gluons were deconfined and thus suffused the entire universe in a thermalized state of quark-gluon plasma [1]. When the value of energy density became below than $1GeV/fm^{-3}$, hadrons were formed out of this state. After the formation of hadrons temperature fell to a value of approximately $100KeV$, stable small nuclei formed. But still the universe is expanding and the temperature is still decreasing. Fig 1.1 is showing the complete change of universe from a state of such a high temperature towards a lower temperature.

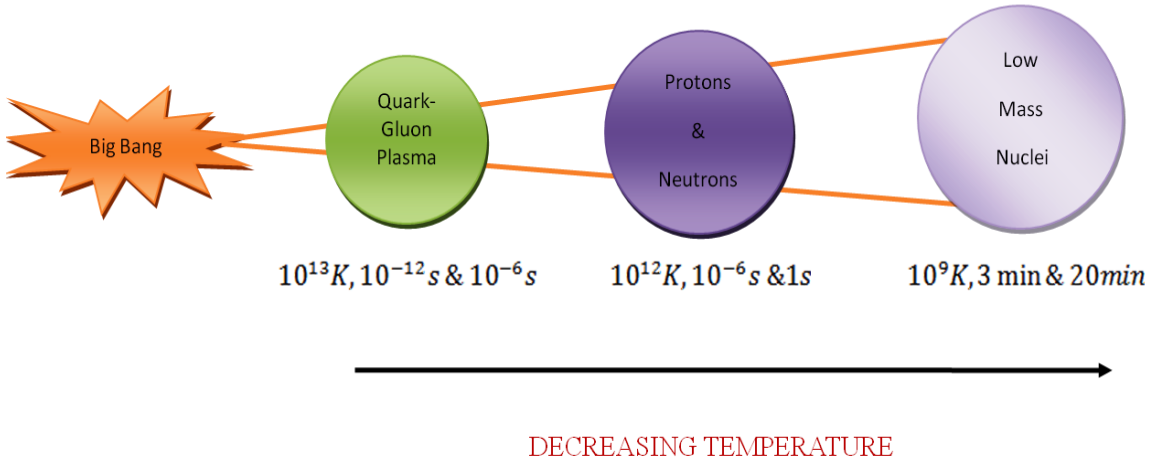

Fig 1.1: Depiction of chronology of universe.

The normal nuclear matter density is of the order of $\rho_0 = 0.17fm^{-3}$ which in terms of mass is equivalent to $10^{27}g/cm^3$ which is a huge number when compared with the surrounding entities. This density can reach up to a higher value when normal nuclear reaction occurs. Since, temperature has a direct proportional relation with density; hence with increase in density, there is exponential increase in temperature. In case of heavy ion collisions, temperature can attain the value upto the units of MeV, which in regular terms is of the order of billions of Kelvin. The Fig 1.2 is showing the phase diagram of hot dense nuclear matter. The temperature is shown along the Y axis while the density is along X axis. When $\rho = \rho_0$, the normal nuclear matter represents a liquid phase. The region of higher temperature represents the quark gluon plasma phase. At intermediate temperature regime, hadron gas phase exists. Hence the concept of temperature is very important in nuclear physics.

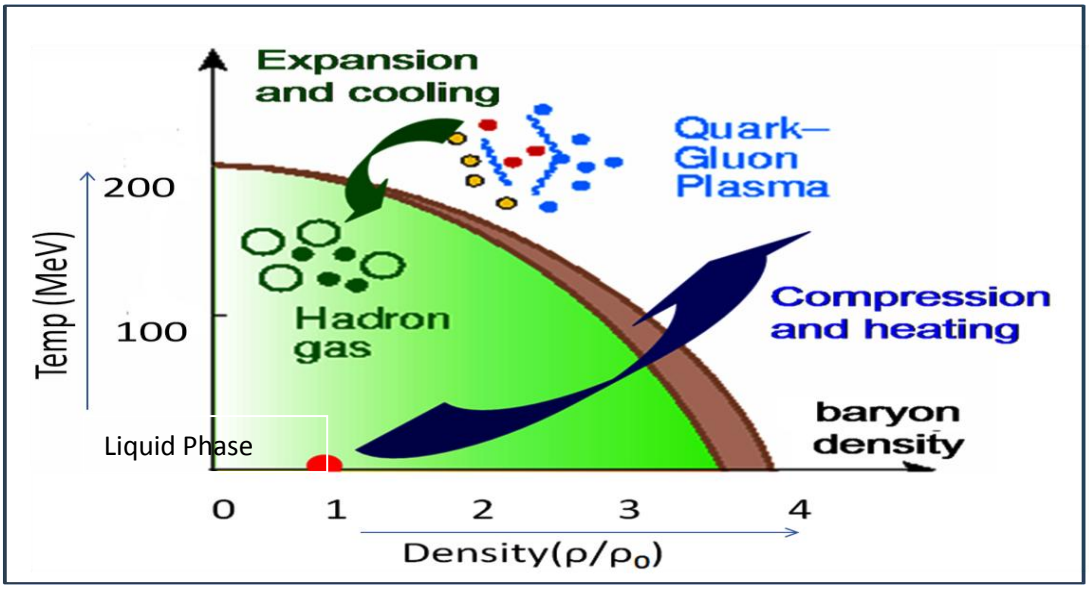

Fig 1.2: Theoretical predicted phase diagram of the nuclear matter.

1.1 Temperature in Heavy Ion Collisions (HICs)

The most impressive feature in the HICs is that the non-equilibrium features of nuclear matter can be studied in the heavy ion reactions. Temperature plays a crucial role in thermodynamic models but yet it is not clear that whether temperature is well defined in such a small systems as are created in heavy ion collisions (HIC) or not [2].

In heavy ion systems, when the energy of projectile beam is increased, the spectator part of the projectile is excited due to the migration of some participant part to the spectator part [3]. At this stage, rather determining the excitation energy as such, a good idea is to determine the temperature. Fig 1.3 is showing the schematic view of heavy ion collision. When the two nuclei collide with each other, a hot dense matter is formed at the central region of the whole system. This hot matter acts like a compressible fluid. At high energies, the nuclear matter tends to squeeze out of the hot compressed zone in the direction orthogonal to the reaction plane. At low energies the nuclear attractive forces start dominating the repulsive thermal pressure and results in the decease of transverse flow.

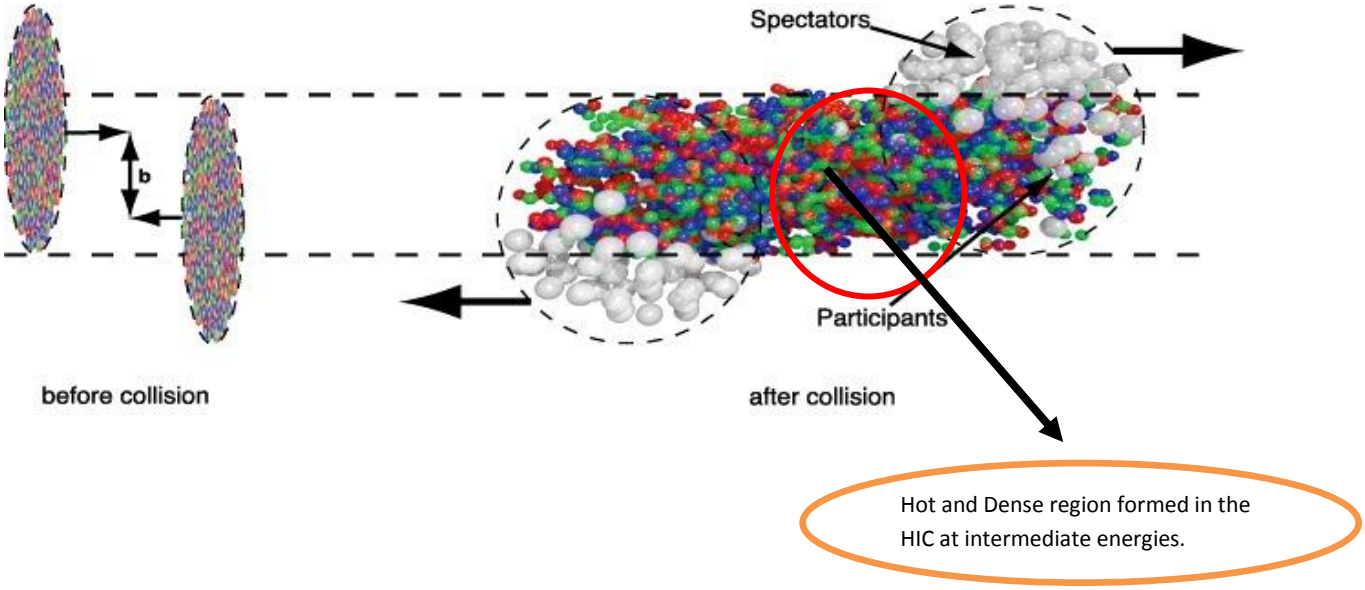

Fig.1.3: schematic view of heavy ion collision.

1.1.1 At low energies

In this energy regime, the properties of the nuclear matter can be studied around the normal nuclear matter density. The phenomenon of fusion dominates the cross-section of HIC at low energies. In this process, whole of the projectile is captured by the target nucleus and the whole of the linear momentum of projectile is transferred to the composite system known as compound nucleus. When two nuclei overlap completely, nuclear density becomes approximately twice of saturation density, and hence the energy density and temperature of the system is increased [4]. From this the variation of increased energy with temperature is calculated.

Below is the Fig 1.4, which is depicting that temperature reached in the HIC at low energies is in the regime of less than 5MeV/nucleon. This energy range is studied at some of the accelerators situated at UNILAC and SIS at GSI in Darmstadt, GANIL in France, CELSIUS in Sweden.

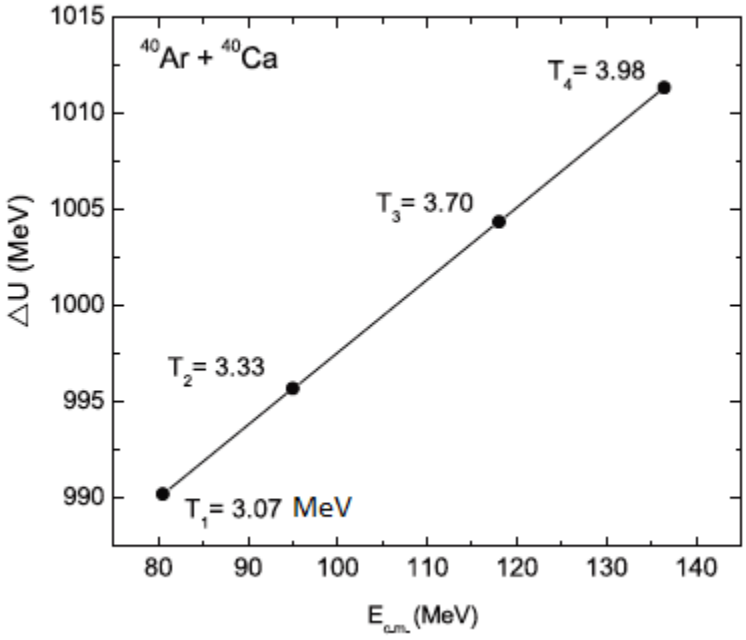

Fig 1.4: Variations of energy due to complete overlap of two colliding nuclei in terms of projectile nucleus energy. The temperature corresponding to each value of energy is also shown [4].

1.1.2 At high energies

The primary focus of this field is the study of heavy-ion collisions, as compared to lower atomic mass nuclei in particle accelerators. At sufficient high energies, these types of collisions produce the quark–gluon plasma. In peripheral nuclear collisions at high energies one expects to obtain information on the electromagnetic production of leptons and mesons.

In the Fig 1.5, the two nuclei collide with each other at t=0, after approximately *t* ~1 fm/c ~3x10^{-24} sec, a super-dense and hot state of quark-gluon matter is created having density approximately 20 times of normal nuclear matter density. This extreme pressure state causes expansion. After a few fm/c (about 10^{-23} sec), the density of the nuclear matter decreases, and hadronic constituents are produced from "chemically freeze out" state. Still the temperature of system is very high, and the system goes on cooling and after a few seconds, density is small enough so that particles stop interacting and "thermal freeze out" reaches. This energy range is studied using accelerators such as LHC heavy ion collider CERN and RHIC at BNL and TEVATRON at Fermi Lab.

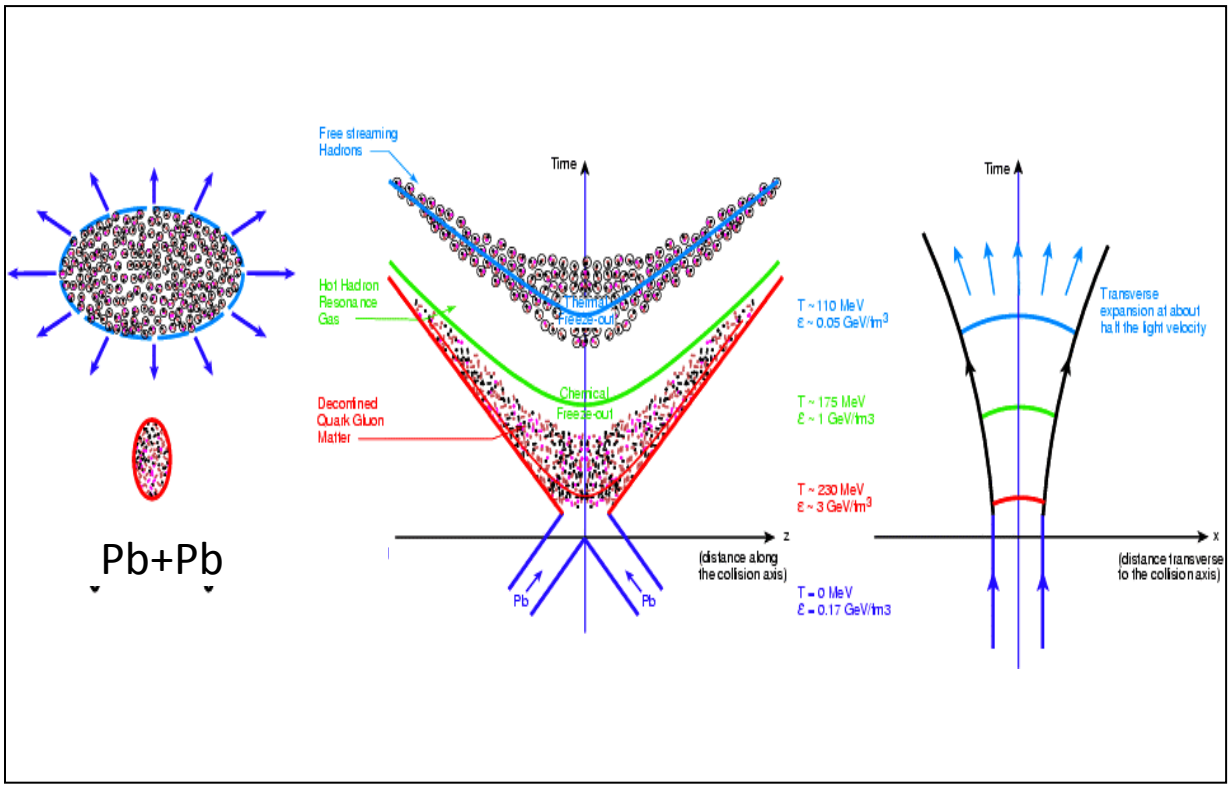

Fig 1.5: Schematic view at high energy nuclear phenomena (E>2GeV/nucleon).

1.1.3 Evolution of temperature in heavy ion collisions (HICs) at intermediate energies

In a nuclear reaction the interaction energy lies in the intermediate regime (50 MeV/nucleon-1 GeV/nucleon), and when two nucleons collide with each other, they suffer various collisions and

form a dense and strongly interacting matter which thermalizes very quickly. This thermalized system has an intense pressure inside it, which leads to the expansion of fireball. As a result of this expansion, the fireball cools and the temperature falls to a lower value due to the disordered motion of nucleons and during this expansion the path traced by this temperature fall is not same. This implies that at a particular value of density, there are two different values of temperature, which means that after collision, the participant matter retains a huge value of temperature even if we try to cool it to its original state. This discussion directly emphasis that the nuclear system, once disturbed takes some time to reach at equilibration stage. During disassembly stage, since the nucleons are parting ways from one another, change in the value of entropy will be small or approximately isentropic process is going to occur after a certain value of density when the system is expanding. Fig 1.6 is justifying the above stated comments. This figure is showing the variation of density$(\frac{\rho}{\rho_0})$, where ρ_0 is the saturation density having the value of $0.16fm^{-3}$ with temperature and entropy per nucleon (S/A).

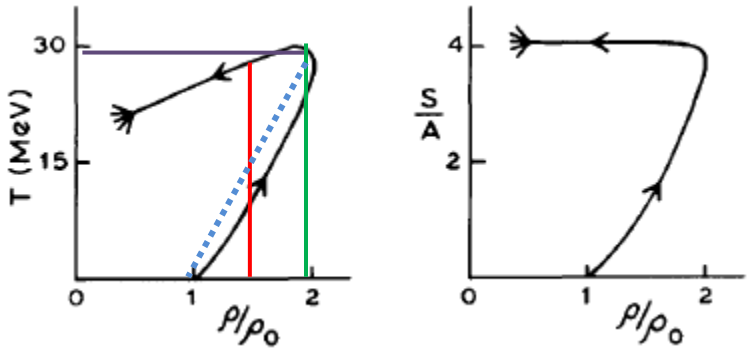

Fig 1.6: A conjecture of the evolution of temperature, density and entropy during the collision [2]

1.2 Methods of Temperature Extraction

Two methods have been suggested in the literature to extract the temperature in HICs [5]. One method is to determine the temperature using kinetic energy spectrum of the fragments while other involves the use of hydrodynamical models and to see does the system reach equilibrium or not.

1.2.1 Study of temperature using kinetic energy spectra

Some of the valuable information about the thermodynamical behaviour can be extracted from the fragment observables experimentally [5]. Nucleons of projectile and target form various fragments. The formation of a fragment depends on the condition defined as

$$|x_i - X_f| \leq R_c \text{ and } |p_i - P_f| \leq P_c \quad \ldots\ldots\ldots\ldots (1)$$

Where (x_i, p_i) represents the i^{th} position and momentum of the nucleons and (X_f, P_f) represents the f^{th} position and momentum of the nucleons. R_c and P_c are the parameters required for the description of fragment multiplicities. In this technique, the methodology used is Seimens and Rasmussen Blast model [6]. The physical significance of this model lies in the fact that the rapid expansion of the hadronic matter leads to a sudden decoupling of hadrons and freezing of their momentum distributions. This model reflects the clear picture of the fireball. In the calculations of fragment kinetic energy spectra, elucidation of kinetic energies is done in the terms of thermalized freeze out configuration. The kinetic energies are given by:

$$\frac{dN}{dE} \sim PE \int \beta^2 d\beta n(\beta) \exp\left(\frac{\gamma E}{T}\right) \times \left[\frac{\sinh\alpha}{\alpha}\left(\gamma + \frac{T}{E}\right) - \frac{T}{E}\cosh\alpha\right] \ldots\ldots\ldots\ldots (2)$$

The spectator part represents the well equilibrated part of a nuclear system. T. Gaitanos et. al [7] shows the time evolution of the local temperature and the density for the spectator in semi-central Au+Au collisions at various incident energies. Their study showed that after the time when the spectator is fully developed the densities and temperatures are independent of incident energy and remain constant for several tens of fm/c. In this experiment, the slope temperatures separately for the fragment of different masses and also the local temperature for comparison are shown. The slope temperatures of the fragments are considerably higher than those of the nucleons saturating for $A_f \geq 3$ around $T_{Slope} \sim 17$ MeV.

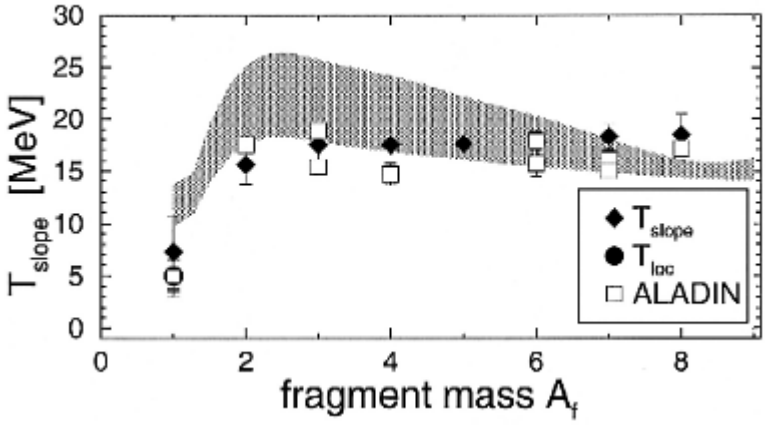

Fig.1.7: Spectator slope temperatures for different fragment masses A_f for the reaction Au+Au. Also shown are the nucleon local temperature (circle) and the temperature obtained from a statistical model (triangle and gray band) [7].

They analyzed that T_{slope} varies from T_{loc} by a significant amount. This is also shown by the ALADIN [8] collaboration. Thus it was concluded that T_{slope} is not a thermodynamic temperature but simulates a higher temperature.

Also the participant matter depicts rather the simple picture of thermodynamical behaviour. Hence the temperature extraction of participant matter is also seen. T. Gaitanos et. al [7] showed that slope temperatures increase and flow velocities fall with fragment mass in contrast to the behaviour for the spectator fragments. A similar behaviour was seen experimentally at $1GeV/$ nucleon in Ref. [9,10] and in calculations in Ref. [11].

1.2.2 Temperature extraction using Microscopic models

The main motive of microscopic models is to determine the properties of the nuclear systems from the basic nuclear interaction. These models are based on the transport phenomena. These models are used to treat the non-equilibrium aspects of temporal evolution of collision. Since in the heavy ion collisions at intermediate energy, no complete equilibration is reached even at t=200fm/c, different models can be used to study the variation of temperature with different parameters. Hydrodynamic models can also be used in the evaluation of temperature, but they

can provide the information mainly on local conditions [12]. In the microscopic study, projectile and target are assumed as the two interpenetrating pieces of nuclear matter and thus the Thomas Fermi approach is used.

D.T. Khoa et. al studied the temperature dependence on various parameters. The variation of maximum and average temperature [13] with time and variation of maximum and average density with time was studied and it has been observed that the maximum values were not much different from that of average ones which directly pointed out that the dense matter is formed in the central region. Also the time at which the maximum temperature reached is approximately same for all the systems [13], since between 10fm/c and 20fm/c maximum numbers of collisions are going to happen and the temperature of the central region is going to reach at its pinnacle. Aftermath, the nuclear matter expands due to lesser number of collisions and due to the outward flow, the temperature of the projectile and target system decreases.

1.2.2.1 Incident energy dependence of temperature

At fixed value of energy, the variation of temperature and density with time was determined respectively. It was then verified that the temperature varies linearly with time. But when a range of energies was checked, the average temperature increases with increase in energy. When energy is decreased, the heating process loses its fast pace, which is also very obvious. When the incident energy is high projectile and target will interact with one another more rigorously as compared to the much smaller value of energy.

1.2.2.2 Impact parameter dependence of temperature

In the central or head on collisions, most of the nucleons fall under the participant zone and the number of collisions are present in a large number and hence more interacting nuclear matter is there. In peripheral collisions, nucleons in the participant zone decreases and nucleons in the spectator zone increases. As a result, number of collisions decreases, and hence nuclear matter density and thus temperature decreases.

The important factor in the study of temperature was to know how fast the equilibration is reached. The direct indicator of equilibration is the anisotropic ratio and entropy. D. T. Khoa et.

al [14] studied that the anomalous decrease of the entropy indicates a break-down of the one-body TF approximation during the decompression stage.

1.2.2.3 Correlation of temperature with nuclear stopping

Nuclear stopping is the measure of converting the incoming energy of the projectile and target into transverse degree of freedom and the nucleons are being slowed down. When projectile and target are boosted towards each other then three pathways can be suggested,

a) Either the nuclei will be repelling each other (full stopping).

b) Either there will be compression or nuclei will tend to mix with one another (stopping and mixing).

c) Either they will not interact or will pass as such without interaction (transparency). Due to such kinds of possibilities, different distributions in longitudinal momenta will take place and for the case of full stopping, initial correlation between the nuclei die out. Nuclear stopping can be used as a probe to extract the information on the isospin dependence of in-medium nucleon-nucleon cross section in intermediate energy heavy ion collisions [16]. Nuclear stopping plays an important role in thermalization. Hence it is also used to determine the temperature.

Anisotropic ratio and Quadrouple moment gives information about nuclear stopping. Since the heavy ion collisions are related to non equilibration effects. And the study of equilibration process is very important.

The anisotropic ratio is related to equilibration process; hence it can be easily related to the temperature. From anisotropic ratio information about global equilibrium can be gained global equilibrium is reached when <Rp> is approximately equal to one. It is given by

$$<R_p>=\frac{\sqrt{p_x{}^2+p_y{}^2}}{2\sqrt{p_z^2}} \quad \text{.....(3)}$$

The anisotropy ratio decreases with increase in the N/Z (neutron to proton) ratio of colliding nuclei because if N/Z is increasing, Z is decreasing, which in turn implies that the strength of Coulombic repulsion decreases, hence the transverse momenta is decreasing and hence $<R_P>$ decreases. The anisotropy ratio increases when incident energy is increased, because as the incident energy increases the transverse momentum increases for head on (central) collisions.

Quadrouple moment is defined as $Q_{ZZ}=\sum_i[2p_z^2\ (i)- p_x^2(i)- p_y^2(i)]$, p_x and p_y are the transverse momentum and Pz represents the longitudinal momentum. When $<R_a>$ is close to one, Q_{ZZ} is close to zero.

S. Gautam et. al [17] showed that temperature is significantly dependent on system's mass. They carried out the simulations for mass symmetric reactions. In their study it has been found that maximal value of$<\rho/\rho_0>$ is higher for lighter systems as compared to the heavier ones. Moreover, the density profile is more extended in heavier systems, indicating that the reaction finishes later in heavier systems. They display the maximal values of T_{avg} and T_{max} as functions of the composite mass of the system. This system-size dependence of temperature reached in the central region is in sharp contradiction to the evolution of density reached in the central region. This is because the temperature depends also on the kinetic energy (i.e., excitation energy) of the system [13, 15].

K. Vinayak et. al [18] showed the variation of nuclear stopping and temperature with impact parameter. With increase in impact parameter, temperature decreases. They carried out their study using Isospin dependent quantum molecular dynamics (IQMD) model.

S. Goyal et. al [19] studied the reaction dynamics for mass symmetric and asymmetric nuclear reactions. They extended their work for the central collisions to see the effect of mass asymmetry of the reaction on the nuclear dynamics at the balance energy. Similar work has been carried out by Sood and Puri [20] for the nearly symmetric and asymmetric reactions at the balance energy, but the role of mass asymmetry in the participant-spectator matter, average and maximum density and temperature, net collisions, anisotropic ratio, relative momentum, and the mass dependence of these quantities was not paid attention. This has been taken care of in the present study. The study was made using quantum molecular dynamics (QMD) model. They observe a notable effect of mass asymmetry on these quantities.

CHAPTER 2

METHODOLOGY

Introduction

The transport models are classified into two categories, one body transport models and many body transport models. They not only provide the information about the initial collisions, but also provides the knowledge about the nuclear equation of state at high density.

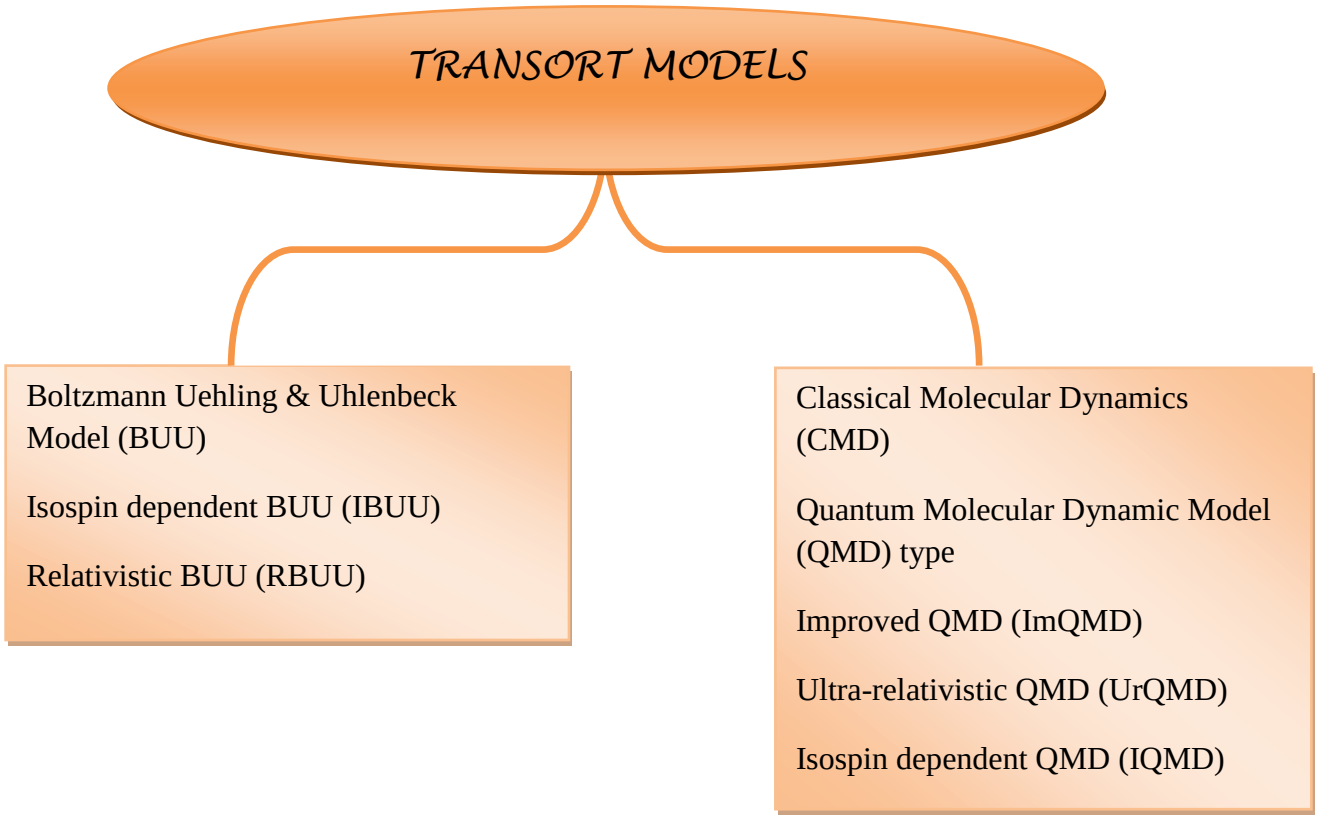

In literature the work on the temperature extraction has been done using both QMD as well as IQMD model. In the present work the methodology of IQMD model is carried out. It is important to know about the Isospin term used in the IQMD model so as to have a look on the advantages of the IQMD model.

2.1 Need of Isospin term

The Isospin term is added in the Quantum Molecular Dynamic Model. Isospin term implicates the exploration of novel phenomena associated with the mass to charge ratio, or neutron to proton, asymmetry of finite nuclei and nucleon matter.

These properties influence the response of nuclei in energetic nuclear collisions, dynamics of supernovae, as well as the structure and evolution of neutron stars. The ultimate goal of this new field is to generate an understanding of nuclear many body systems in terms of an Isospin dependent nuclear equation of state and in medium nucleonic interactions. The Isospin degree of freedom enters into the calculations via both cross-sections and the mean field [21,22]. The IQMD [23] model is a successful model for explaining the analysis of large number of observables from low to relavistic energies [24].

In the present work, the basic methodology used will be Hot Thomas Fermi approach. Out of various transport models [25], Isospin Quantum Molecular Dynamic Model (IQMD) will be used to study the thermal properties of nucleons involved in Heavy Ion Collisions (HIC).

2.2 The hot Thomas Fermi Formalism

In hot Thomas Fermi approach [15], each local volume element of nuclear matter in coordinate space and time has some temperature defined by the diffused edge of deformed Fermi distribution in HIC. In the hot nuclear matter at temperature (T), the momentum distribution of nucleons is given by the Fermi-Dirac distribution

$$n(k) = \frac{1}{1+\exp(E(k)-\mu)/T} \quad \text{.....(1)}$$

Where E(k) is the energy of nucleon with momentum k μ is the chemical potential determined by normalization of the density of given nuclear matter, T is the temperature. From this the kinetic energy and entropy is measured.

$$\rho = \frac{g}{(2\pi)^3}\int_F n(k)dk \ldots\ldots\ldots (2)$$

$$\tau = \frac{g}{(2\pi)^3}\int_F k^2 n(k)dk \ldots\ldots\ldots (3)$$

g is the spin-Isospin degeneracy of a nucleon with momentum k, F is the diffused Fermi sphere

and an effective mass approximation is used which give rise to mean field theory. But actually $F=F_1+F_2$, separated by K_R, the relative momentum. Initially K_R is very large, as the projectile and target collides, the relative velocity decreases and as a result of it K_R decreases. The relative momentum never becomes zero as the projectile and target tend to expand. Hence it is a necessary to consider the deformed momentum distribution.

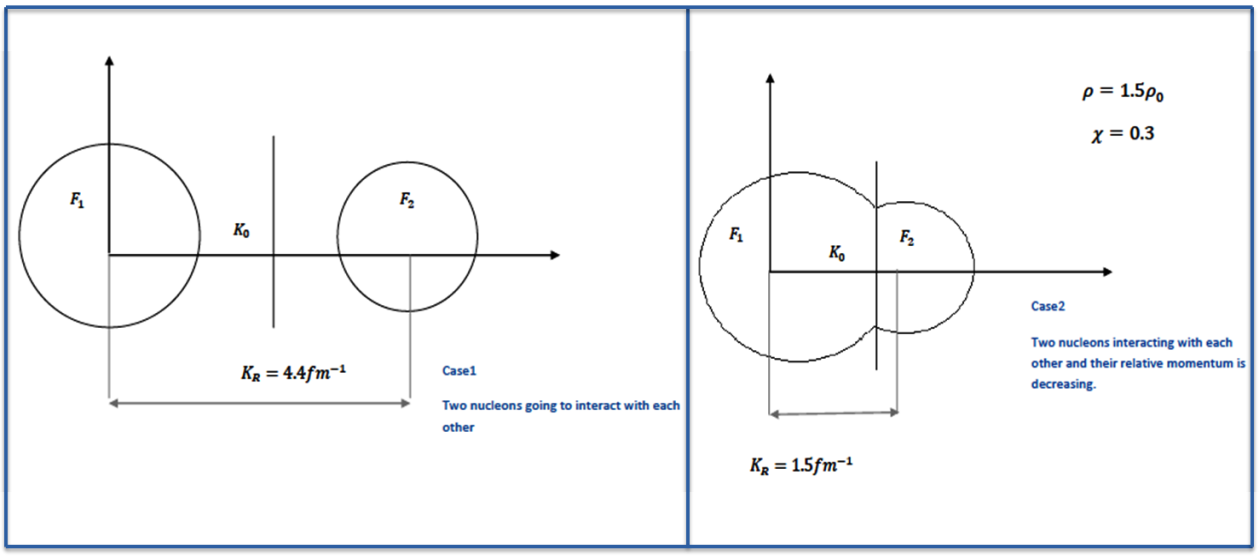

Fig. 2.1: Momentum distribution of two nucleons in two colliding spheres separated by their relative momentum K_R with total density 1.5 times the normal nuclear matter density.

The total density is kept at the same scale because there exists a limit on the two spheres given by the Pauli's exclusion principle.

To avoid the overlap, density is kept at same scale. The momentum distribution of nucleons in a heavy ion collision in two Fermi spheres at rest frame is calculated from the Fermi sphere having higher density.

$$n_1(K_r, K_z) = \frac{1}{1+\exp\left[\hbar^2\left(K_r^2+K_z^2\right)\frac{1}{2*m*T-\eta_1}\right]} \quad if\ K_z < K_0 \text{ ……..... (4)}$$

$$n_2(K_r, K_z) = \frac{1}{1+\exp\left[\hbar^2\left(K_r^2+(K_z-K_R)^2\right)\frac{1}{2*m*T-\eta_2}\right]} \quad if\ K_z \geq K_0 \text{ …… (5)}$$

With $$K_0 = \left[{K_R}^2 - 2 * m * T(n_1 - n_2)\right]/2K_R \text{ …… (6)}$$

K_0 is chosen in such a way so that $n(K)$ should be a continuous function in K. n_1 and n_2 are calculated through the normalized matter densities of the two colliding spheres.

2.3 ISOSPIN QUANTUM MOLECULAR DYNAMIC (IQMD) MODEL

The IQMD model was developed by Hartnack et al. [23]. Its principle is same as that of QMD [27, 28] but an extra Isospin term is being taken into account. In IQMD different charge states of nucleons has been treated explicitly. Both the cross-section and mean field are included in IQMD. The term Isospin used in IQMD affect the elastic and inelastic cross-sections. It is described by three steps

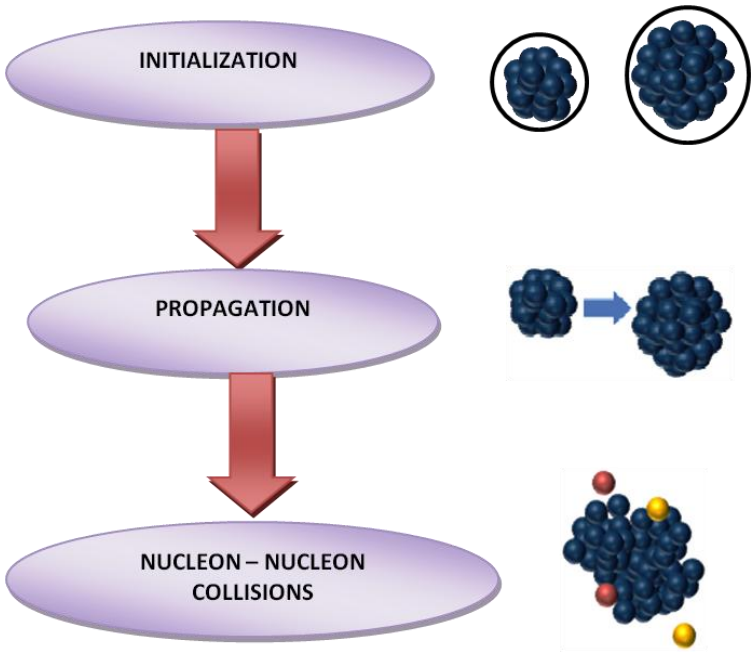

2.3.1 Initialization of nucleons

For every process, first one must initialize the nucleon and the wave function of the nucleon Initialization is quite different from that of QMD in the manner that in IQMD, Fermi momentum depends on ground state density, whereas in QMD Fermi momentum depends upon local potential and hence a stronger stability of density profile is determined. In IQMD model, a nucleon is represented as a Gaussian wave packet which interact by mutual two bodies and three body forces. The simulations are executed on an event by event basis, and so the fluctuations and correlations are preserved. The wave function of the i^{th} nucleon having mean position $r_i(t)$ and mean momentum $p_i(t)$ is represented as

$$\psi_i(r, r_i(t), p_i(t), t) = \frac{1}{(2\pi L)^{3/4}} \exp\left[\frac{i}{\hbar} p_i(t).r - \frac{(r - r_i(t))^2}{4L}\right] \quad \ldots\ldots\ldots\ldots (7)$$

The parameter L provides the mensuration for the interaction range of nucleons. In IQMD model L depends on the size of the system. The mass dependence of L is included so as to provide, the better density stabilization. For heavy system $(Au + Au)$ L=8. 66fm^2 whereas for a lighter system $(Ca + Ca)$, it is about 4.33 fm^2. The value of radius is taken as R= 1.2 A$^{1/3}$ fm. The total wave function can be thus represented as

$$\Phi = \prod_i \ \psi_i(r, r_i, p_i, t) \quad \ldots\ldots\ldots\ldots (8)$$

But since the semi classical theory has been taken into account, hence instead of wave functions, Wigner representation is used. The Wigner representation of a system (containing Projectile and Target) is given as

$$f_i(r, p, t) = \frac{1}{\pi^2 \hbar^2} e^{-(r - r_i(t))^2 \frac{1}{2L}} e^{-(p - p_i(t))^2 \frac{2L}{\hbar^2}} \quad \ldots\ldots\ldots\ldots (9)$$

This Wigner distribution obeys the well known Heisenberg's uncertainty principle i.e.

$$\Delta x . \Delta p \geq \hbar/2 \quad \ldots\ldots\ldots\ldots (10)$$

For initialization of nucleons, it is necessary for the nucleons to have the proper assigned position and momentum coordinates. A three dimensional sphere having $R = 1.12A^{1/3}$, whereas A is the mass number of the nucleus under consideration.

Initialization of Position Coordinates

The centers of Gaussian wave packet r_i are uniformly distributed in polar coordinates by

$$r = R x_1^{\frac{1}{3}} \quad \ldots\ldots\ldots\ldots\ldots\ldots (11)$$

$$cos\theta = 1 - 2x_2 \quad \ldots\ldots\ldots\ldots (12)$$

$$\phi = 2\pi x_3 \quad \ldots\ldots\ldots\ldots\ldots\ldots (13)$$

x_1, x_2, x_3 are random numbers. If the distance between the nucleons is less than $1.5fm$, coordinates are rejected. The volume of a nucleon is so adjusted ($V_{single\ nucleon} = h^3$) Such that the phase space gets uniformly filled.

Initialization of Momentum Coordinates

Momenta of a nucleon is taken between 0 and p_f, where p_f depends on the ground state density.

$$p_i = p_f(r_i)x_4^{\frac{1}{3}} \quad \ldots\ldots\ldots\ldots\ldots\ldots (14)$$

$$\cos\theta = 1 - 2x_5 \quad \ldots\ldots\ldots\ldots\ldots\ldots (15)$$

$$\phi = 2\pi x_6 \quad \ldots\ldots\ldots\ldots\ldots\ldots (16)$$

To have a more tranquil distribution of nucleons in a phase space, nucleons have to satisfy a particular constraint

$$|r_i - r_j|^2 |P_i - P_j|^2 \geq d_{min} \quad \ldots\ldots\ldots (17)$$

Out of approximately 50,000 initializations [29] only one is accepted. As the incident energy increases Lorentz contraction becomes important.

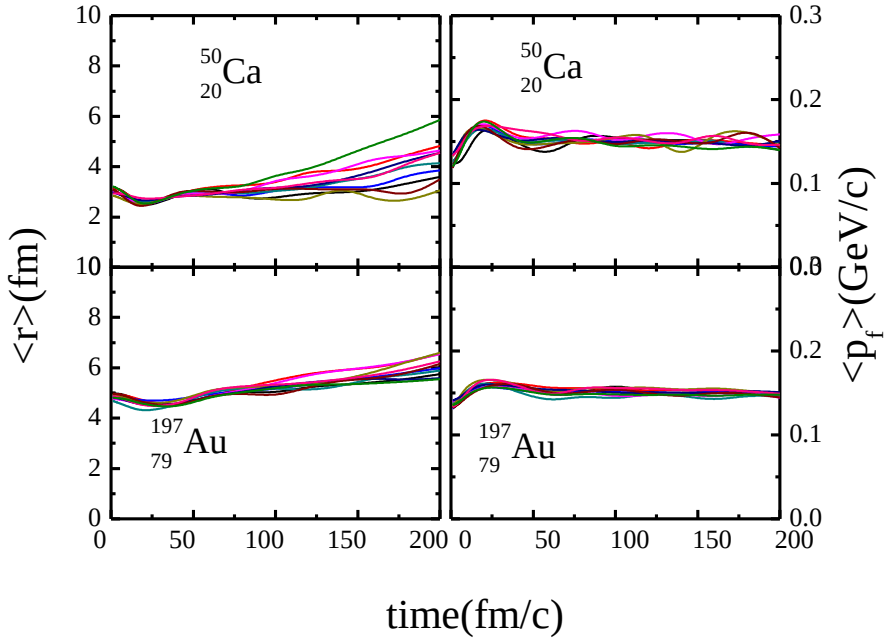

Fig.2.2: Time evolution of the root mean square radius and momentum. For each nucleus we display the radius and momentum for ten different initializations.

Fig 2.2 is showing the time evolution of the radii (left panels) and momentum (right panels). In the case of heavy nuclei, the oscillations are being observed around the mean value but no emission of nucleons occurs. For the lighter system, as in the case of $^{50}_{20}Ca$, the nucleus is less stable and can emit nucleons easily.

2.3.2 Propagation of nucleons due to their mutual potential interaction

Later on the initialized nucleons are made to propagate with proper center of mass velocity using relativistic kinematics. The isospin degree of freedom is handled explicitly by using a symmetry potential and explicit Coulomb forces between protons of colliding target and projectile. The propagation of nucleons are given by Hamilton's equations of motion.

$$\frac{\partial r_i}{\partial t} = \frac{\partial <H>}{\partial p_i} \quad \text{..... (18)}$$

$$\frac{\partial p_i}{\partial t} = -\frac{\partial <H>}{\partial r_i} \quad \text{..... (19) , where <H> is the Hamiltonian}$$

The nucleon- nucleon interaction is given by the potential

$$V^{ij}(r' - r) = V^{ij}_{Skyrme} + V^{ij}_{Yukawa} + V^{ij}_{Coul} + V^{ij}_{Mdi} + V^{ij}_{Sym}$$

$$= \left(t_1\delta(r' - r) + t_2\delta(r' - r)\rho^{\gamma-1(r'+r/2)}\right)$$

$$+t_3\frac{(\exp(|r' - r|/\mu))}{(|r' - r|/\mu)} + \frac{Z_iZ_je^2}{|r' - r|} + t_4 ln^2\left[t_5\left(p_i' - p\right)^2 + 1\right]\delta(r' - r)$$

$$+ t_6\frac{1}{\varrho_0}T_3^iT_3^j\delta\left(r_i' - r_j\right) \quad \text{..... (20)}$$

Here Z_i and Z_j denote the charges of i^{th} and j^{th} baryon, and T_3^i , T_3^j are their T_3components respectively (1/2 for protons and -1/2 for neutrons). $\mu, t_1, \ldots\ldots\ldots\ldots, t_6,$ are so adjusted so as to get the real part of nucleonic optical potential. Yukawa potential stabilizes the surface of finite nucleus. Meson potential has Coulomb interaction only. V_{Skyrme}^{ij} and V_{Mdi}^{ij} are Isospin independent. For the density dependence of nucleonic potential skyrme type parameterization is employed and hence soft and hard nuclear EOS are being used and fluctuations are thus reduced.

2.3.3 Nucleon-Nucleon collisions

The nucleon-nucleon collisions are treated in the same manner as in the cascade model.

Nucleons suffer collisions only if

$$|r_i - r_j| \leq \sqrt{\frac{\sigma_{tot}}{\pi}}, \sigma_{tot} = \sigma\left(\sqrt{s}, type\right) \ldots\ldots\ldots\ldots\ldots (21)$$

Where "type" in equation denotes the ingoing collision partners (N-N, N-Δ, N – π etc.). The colliding particles can also scatter elastically or inelastically. Fig 2.3 is showing the trajectory of a nucleon suffering collision at different time steps.

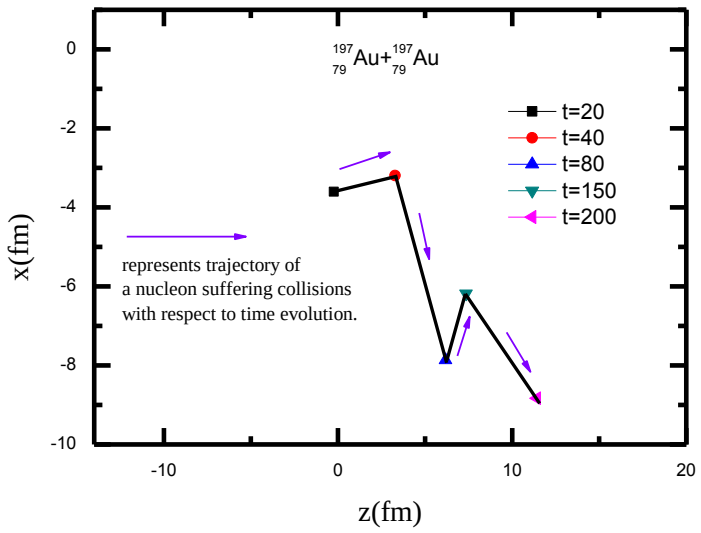

Fig.2.3: Phase space of a nucleon in Au+Au system suffering collision at different time steps.

2.3.3.1 Pauli Blocking

Since nucleons are fermions and hence Pauli Exclusion Principle should be surely applicable to them. But here classical approach is employed; hence the rule has to be changed. Here the concept is that the nucleons must not be present in the overpopulated areas of phase space. The final phase space fractions P_1 and P_2 which are already occupied by other nucleons are determined for each of the scattering baryons. Hence the collision between the two nucleons gets Pauli blocked with the probability as $P_{block}=(1-P_1)(1-P_2)$. And is allowed with probability of $P = 1 - P_{Block}$. Fig 2.4 is showing the time evolution of blocked and allowed collisions for ${}^{50}_{20}Ca + {}^{50}_{20}Ca$ and ${}^{197}_{79}Au + {}^{197}_{79}Au$.

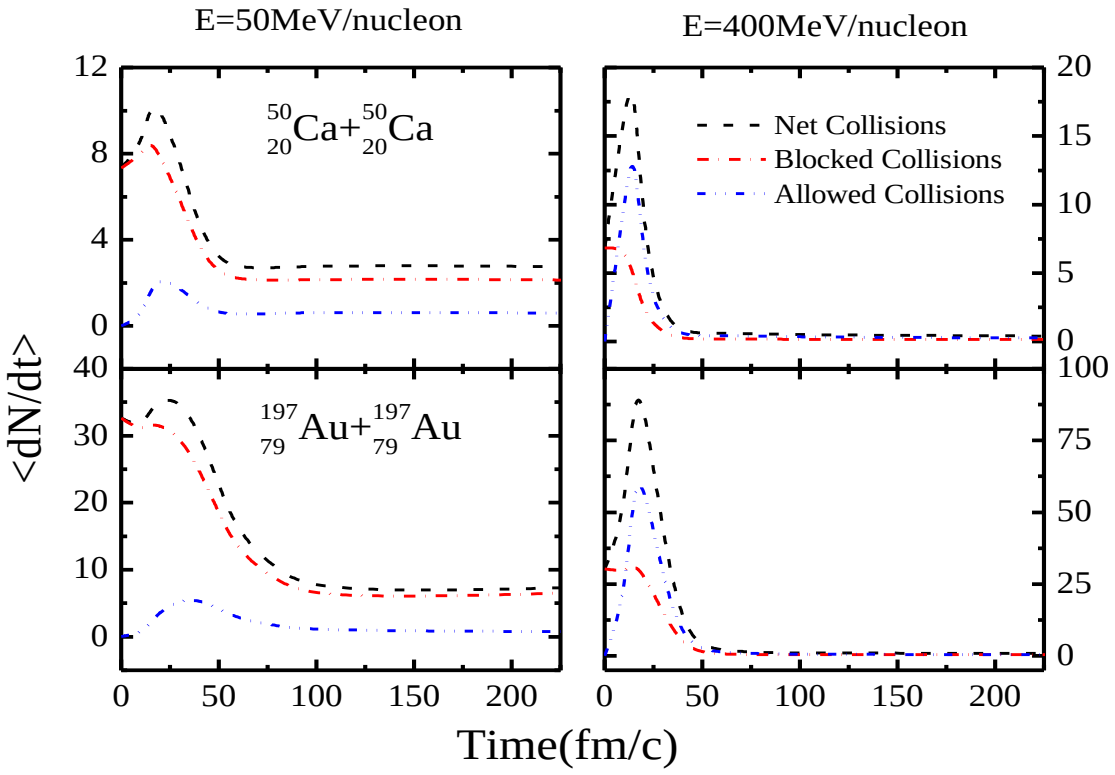

Fig.2.4: The rate of allowed, blocked and net collisions versus the reaction time for the reaction Au+Au.

Since we are talking of collisions, cross-sectional term should be taken into account and the total cross-section is defined as

$$\sigma_{total} = \sigma_{elastic} + \sigma_{inelastic}$$

Inelastic collisions are due to the following reactions.

a) $N + N \rightarrow \Delta + N$ (Hard delta production)

b) $\Delta \rightarrow N + \pi$ (Delta decay)

c) $\Delta + N \rightarrow N + N$ (Delta absorption)

d) $N + \pi \rightarrow \Delta$ (Soft delta production)

For a) and d) [30], cross-sections calculated from experimental data are calculated and for b) and c) [31] information can be extracted from their reverse counter-parts. In IQMD, two different parameterizations are used for N-N cross-sections; one is isospin independent while other is Isospin dependent [32]. Fig.2.5 is showing the time scale of the collisions suffered by the nucleons in the nuclear reaction under the frame work of IQMD.

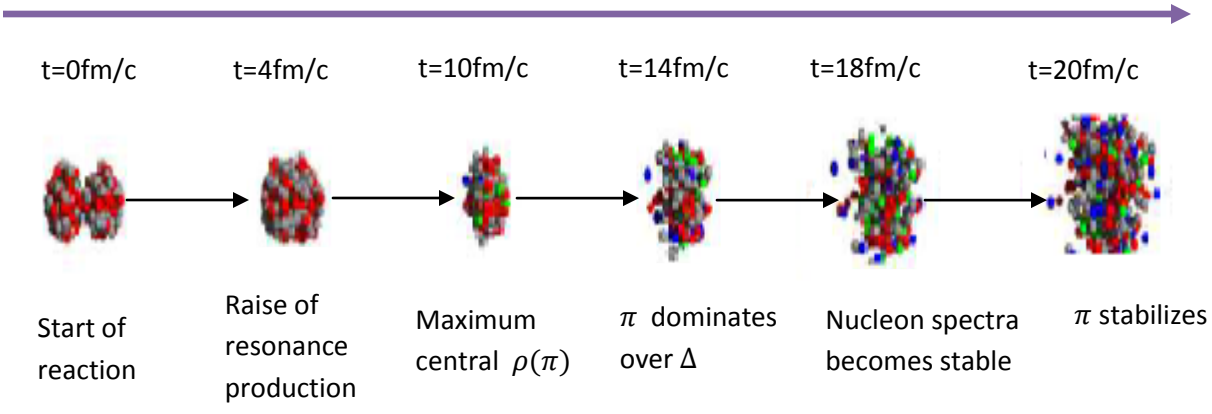

Fig.2.5: Schematic view of the basic scale of time evolution in IQMD model.

CHAPTER 3

STUDY OF TEMPERATURE IN NUCLEAR REACTIONS

3.1 Mass Asymmetry

In nuclear physics two types of reactions are possible, mass symmetric and mass asymmetric reactions. In mass symmetric reactions, the total number of nucleons present in the projectile is equal in number to that of the number of nucleons in the target nuclei. In mass asymmetric reactions, there are unequal number of nucleons in target and projectile. The fig 3.1 is showing the different phenomena occurring in a mass symmetric and mass asymmetric reaction. In mass symmetric reaction, the dynamics of reaction is violent, and along with many small clusters, free nucleons are also emitted. In mass asymmetric reaction, the heavier and less numbers of clusters are produced, along with some free nucleons.

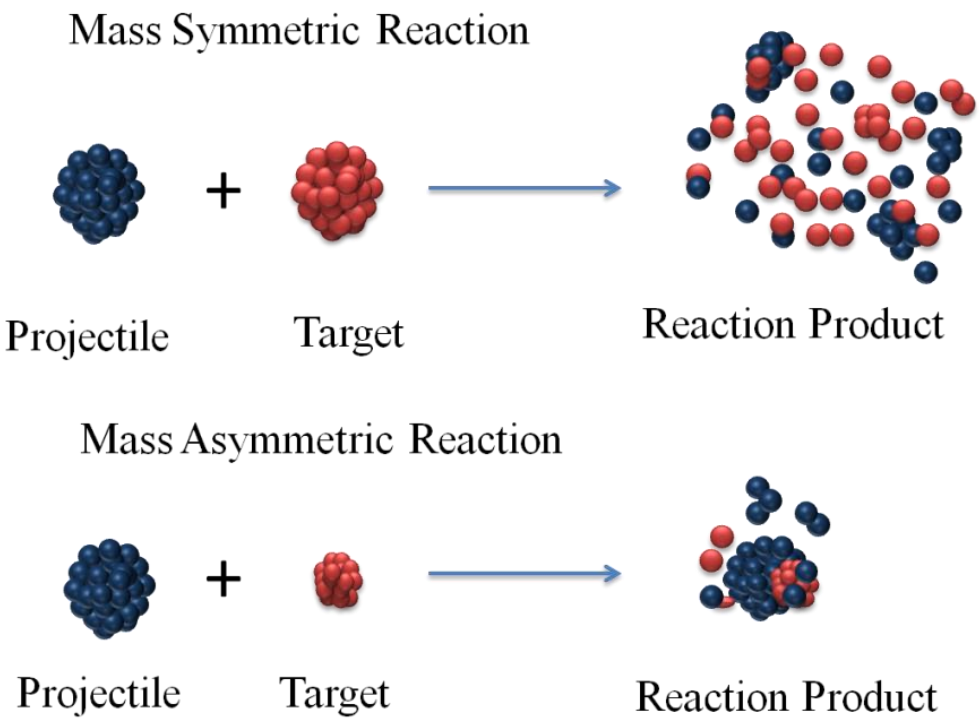

Fig 3.1: Schematic view of the mass symmetric and mass asymmetric reactions.

The mass asymmetry parameter is given as

$$\eta = \frac{A_T - A_P}{A_T + A_P}$$

A_T and A_P are the masses of target and projectile respectively.Fig 3.2 is showing the formation of fragments emitted in the asymmetric reaction. The size of fragments increases with increase in mass asymmetry.

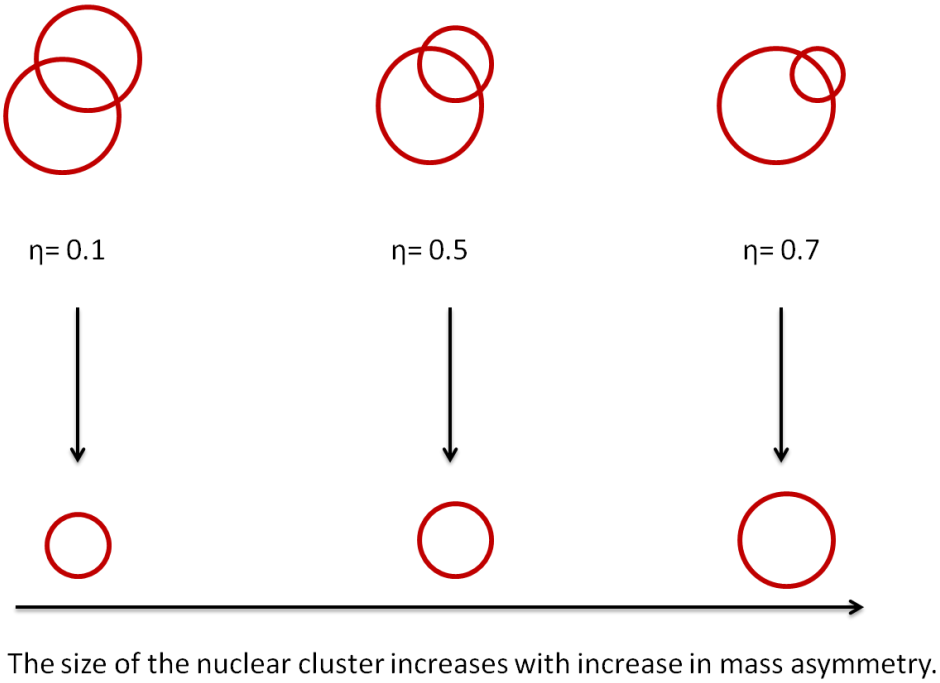

Fig 3.2: Schematic view of the nuclear fragments formed in the mass asymmetric reactions.

Asymmetry of a reaction plays crucial role in heavy-ion collisions. Because, when the two symmetric nuclei collide, a large compressed zone is formed. On the other hand, for the case of asymmetric reactions, due to the difference between the masses of the projectile and target, the nucleons of the projectile and the target are not able to interact with each other. Hence a lesser compressed zone is formed in the asymmetric collisions.

3.2 Introduction to mass asymmetry in HICs at intermediate energies

The quest for the study of the asymmetric reactions became important after successfully operating dynamics of symmetrically colliding nuclei, both in experimental and theoretical studies. An experiment was concluded by Betts [33] in 1981 in which he measured the fusion probabilities for different colliding pairs which led to the formation of same compound nucleus. Then Liu studied the Isospin effects on the process of multifragmentation and dissipation by considering the asymmetric colliding pairs. In 2010, Kaur et. al [34] studied the simulations of various asymmetric nuclei and took a particular range of mass asymmetry (η) ranging from -0.8 to +0.8 and showed that as η shifts towards the positive side, the target fragmentation takes place, since $A_T > A_P$ and as η shifts towards the negative side, the projectile fragmentation takes place. They also studied the effect of Coulomb interaction for these reactions. However, the coulomb interaction decreases with energy, its effect remains almost constant with asymmetry of the reaction. They extended their study for extracting the values of the anisotropic ratio (R) and quadruple moment (Q_{ZZ}). They kept the total mass fixed and vary the value of asymmetry from η=0 to η=0.7. They concluded that with increase in η both R and Q_{ZZ} increases, since for the two asymmetric colliding nuclei there is decrease in the longitudinal momenta. In 2011, another study by Goyal et. al revealed the effect on the collective transverse flow for different mass asymmetries as a function of impact parameter [35]. And it was concluded that geometry of vanishing flow provides an enough good sensitivity to the mass asymmetry. In 2012, kaur et. al extended the work in HICs by studying the effect of Isospin independent cross section (σ_{noiso}) in comparision to σ_{iso} and they observed a considerable effect of cross section on asymmetric systems [36]. They also compared their data with the experimental data generated by ALADIN collaboration. It came out to be in accordance to the experimental data. In 2012, Gautam et. al studied the participant – spectator matter, density and temperature reached in HIC's of neutron rich systems having different N/Z ratio at different energies [37]. They carried out the simulations for symmetric pair of colliding nuclei. They showed that at higher incident energies the participant – spectator matter is not dependent on the neutron content of the colliding systems. They also studied the temperature N/Z dependence of temperature reached in the heavy ion reaction. This led to the conclusion that the effect of neutron content was almost negligible on the different parameters as described above.

In 2012, Vinayak et. al studied the dependence of temperature with reaction time for different symmetry energies for fixed value of scaled impact parameter $\hat{b}$ using IQMD model. It was concluded that global nuclear stopping gives a good approximation of temperature of nuclear matter formed in the heavy ion collisions. In 2014, K.S. Vinayak et. al studied the reaction dynamics and interplay of density dependent symmetry energies for asymmetric reactions. They concluded the results that the effect of mass asymmetry on the density and the temperature increases with the incident energy of the reaction. It also affects the reaction dynamics at the central collisions. In 2014, S. Goyal et. al studied the temperature and density dependence on mass asymmetry. A notable effect of mass asymmetry on the reaction dynamics was studied using QMD model.

3.3 Rotational Effect

Depending on the impact parameter of the colliding nuclei, the type of the reaction differs. The reaction can be central, semi peripheral or peripheral. In low energies, central collisions lead to fusion, (compound nucleus formation or fast fission) whereas deep inelastic collisions are associated with the peripheral collisions. At high bombarding energies, central collisions lead to the complete explosion of the system, whereas more peripheral collisions are interpreted as fragmentation processes. For peripheral collisions, the target and projectile barely touch each other and moreover, if an asymmetric reaction is considered, the lighter system tends to rotate around the heavier system. Fig. 3.3 is showing how the rotational effect appears into the picture when the impact parameter is increased. This rotational effect can be seen for the mass asymmetric colliding pairs, since in the symmetric colliding nuclei, this effect is absent due to more violent phase of collisions. This can be seen by comparing the phase space of mass symmetric systems with that of mass asymmetric systems.

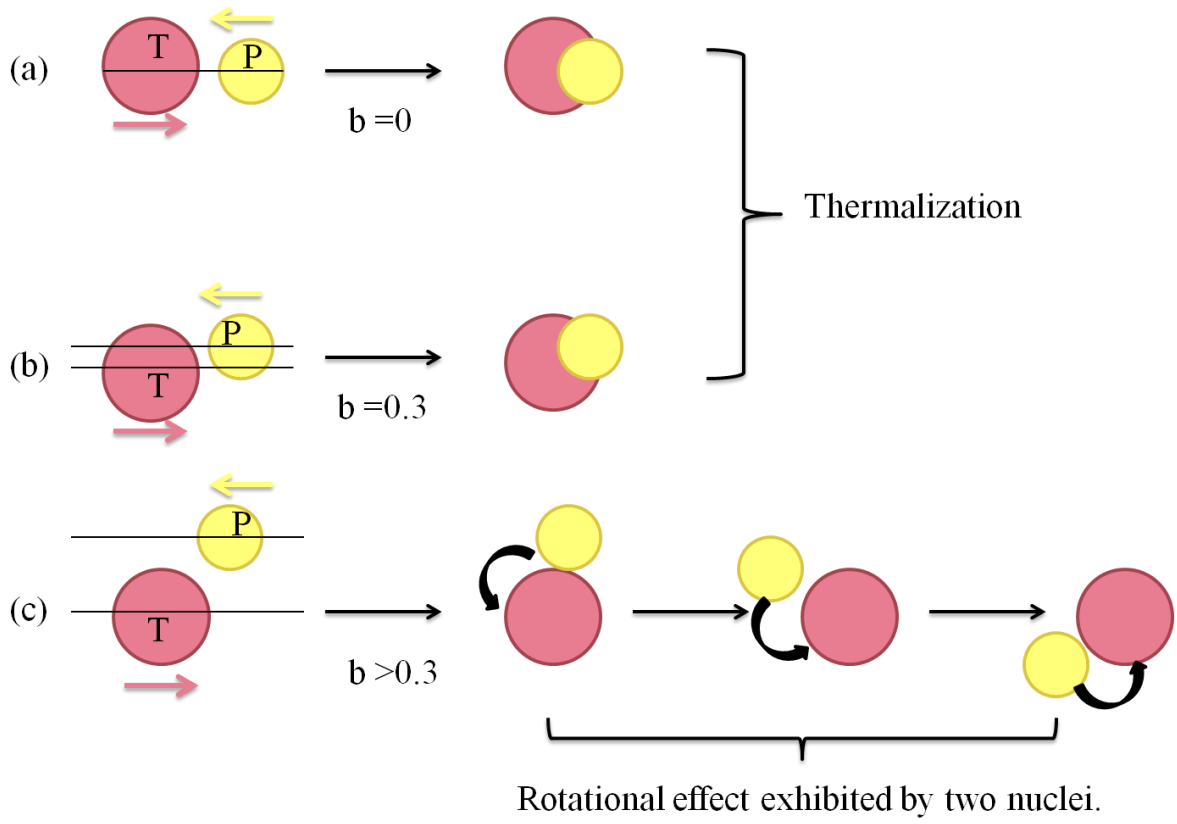

Fig 3.3: Schematic view of the two asymmetric colliding nuclei at different impact parameters.

In figure 3.3(a), collision between the projectile and target is purely central. The nucleons of target and projectile will get enough volume to interact with each other and thermalization will take place. In figure 3.3(b), the value of impact parameter is increased and thermalization will take place to a lesser extent to that of the former case. In figure 3.3(c), as the value of impact parameter is further increased, the projectile will tend to rotate around the target.

3.4 Phase Space

The phase space is an imaginary six dimensional space made up of three spatial components and three momentum components.

The phase space of a nucleus provides enough good information about the trajectories of the nucleons and about the stability of the nuclei. The coordinate space can be studied in X-Y (top view), X-Z (side view).

3.4.1 Phase space of a single nucleus

The Fig 3.4 is showing the snap shots of phase space for the single nuclei $^{197}_{79}Au$. These snap shots are showing the stability of the nuclear matter.

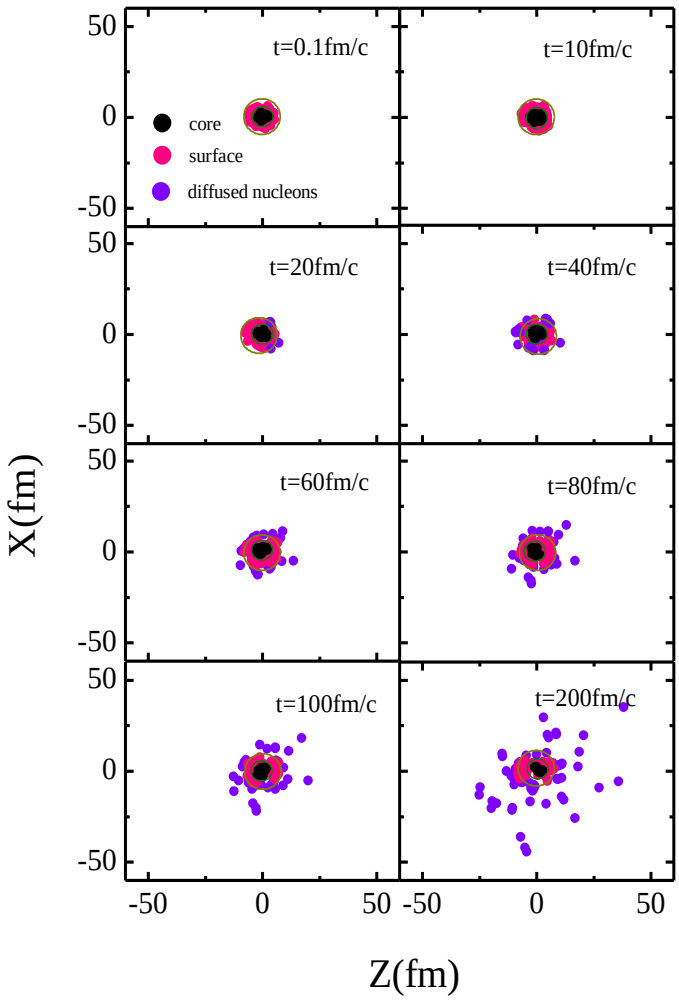

Fig 3.4: Phase space of a single nucleus of $^{197}_{79}Au$. The two areas, namely core and surface are shown.

The phase space is showing the time evolution of the nucleons of the system. It is constructed using the concept of the nuclear radius and nuclear density. To characterize the drop in the density, the concept of surface layer thickness (t) is used. This quantity is defined as the thickness of a layer, across which the density ρ drops from 0.9 to 0.1. of the value at the centre of the nucleus. The data regarding the separation of core and surface of a nucleus is collected from the de Vergis, de Jager, and de Vries (Atomic Data and Nucl. Data Tables, 36, 495, (1987). The phase space is constructed using the IQMD model. At t=0.1fm/c and at t=10fm/c, the system is stable, at t=20fm/c the nucleons from the surface of the nucleus, goes into the diffused space. As the time approaches t=60fm/c, the nucleons from the core, also get scattered. As the saturation time increases, the numbers of nucleons in the core of the nucleus are same as that of the nucleons present in the core at t=0.1fm/c. This study is carried out using IQMD model. Hence, it is concluded that maximum stability of a nucleus is in the vicinity of reaction time, t=10fm/c to t=20fm/c.

The dynamical properties of nucleons can be discussed by studying their phase space. The rotational effect has been picturized by comparing the phase space of both symmetric and asymmetric reactions in Fig 3.5 and Fig 3.7. For this we have simulated a single event for the reaction of ${}^{50}_{20}Ca + {}^{50}_{20}Ca$ (η=0) and ${}^{14}_{7}N + {}^{86}_{36}Kr$ (η=0.7) at E=100MeV/nucleon for impact parameter ($\hat{b}$ =0.7).

3.4.2 Phase space of two mass symmetric nuclei

The phase space of the two nuclei for both symmetric and asymmetric reactions is shown so that we can see that how the phase space is affected. The fig 3.3 shows the phase space of ${}^{50}_{20}Ca + {}^{50}_{20}Ca$ having the total mass=100. In the coordinate space of ${}^{50}_{20}Ca + {}^{50}_{20}Ca$, as the reaction proceeds further, the projectile (${}^{50}_{20}Ca$) and target (${}^{50}_{20}Ca$) tends to overlap with each other. Here the front view is presented.

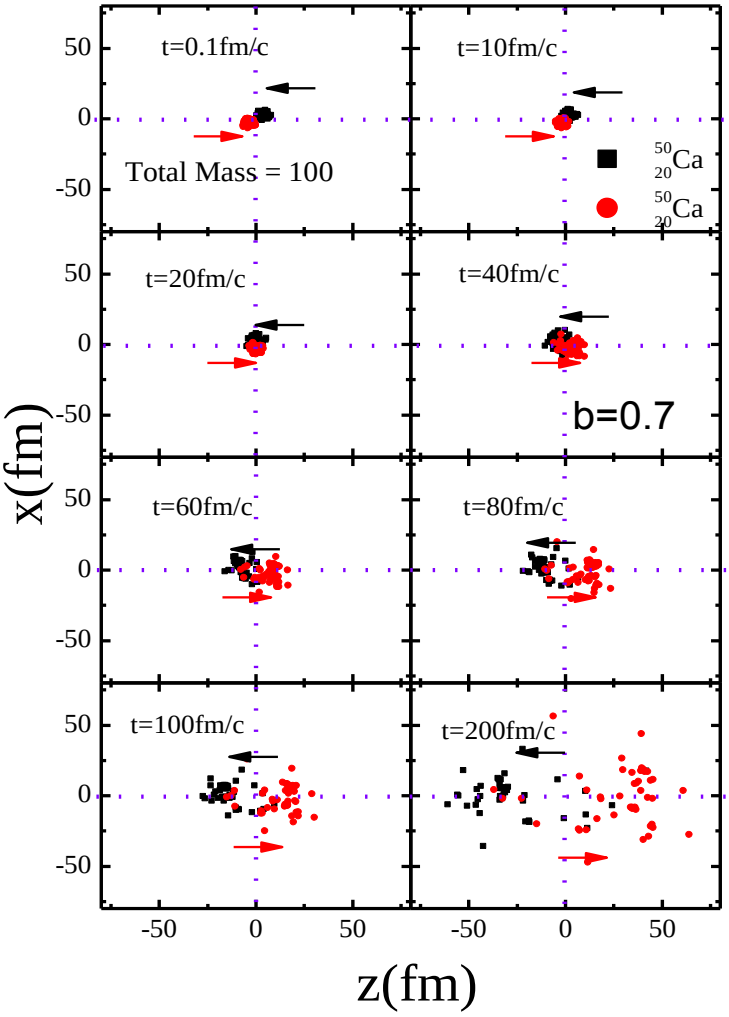

Fig 3.5: Phase space of $^{50}_{20}Ca + ^{50}_{20}Ca$ at $E = 100MeV/nucleon$ and impact parameter, $\hat{b} = 0.7$.

At t=0.1 fm/c the projectile and target are properly initialized and boosted towards each other from each other. As the reaction time is increased, the nucleons of both the projectile and target start to interact with each other due to the enough amount of energy given to the nuclei. And subsequently as the time approaches the saturation point i.e. at t=200fm/c, either the emission of fragments or nucleons will take place. The momentum space is not affected much and hence no

substantial change in the momentum space has been observed. In case of symmetric reaction due to equal distribution of energy among the nucleons, the momentum distribution is uniform.

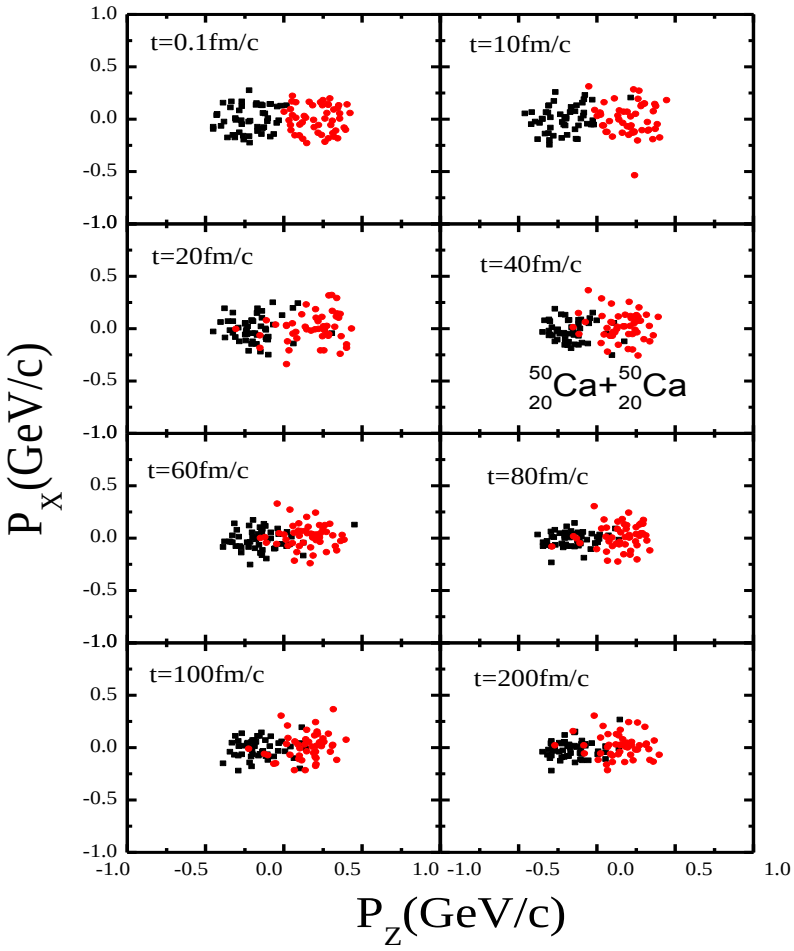

Fig 3.6: Momentum space of $^{50}_{20}Ca + ^{50}_{20}Ca$ at $E = 100MeV/nucleon$ and impact parameter, $\hat{b} = 0.7$.

3.4.3 Phase space of two mass asymmetric nuclei

While for in the coordinate space of $^{14}_{7}N + ^{86}_{36}Kr$, the projectile ($^{14}_{7}N$) tends to rotate about the target ($^{86}_{36}Kr$) and as the time reaches 60fm/c, the various processes occurring in heavy ion collisions like multifragmentation, emission of free nucleons etc. can be seen.

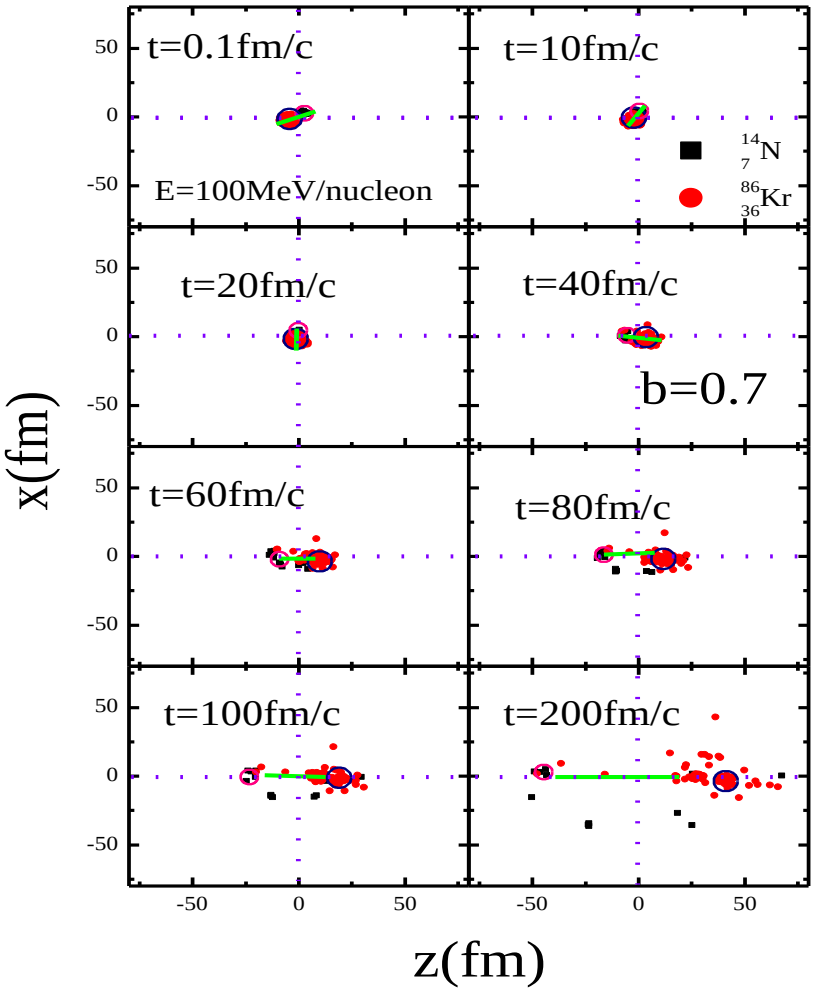

Fig 3.7: Phase space of $^{14}_{7}N + ^{86}_{36}Kr$ at $E = 100MeV/nucleon$ and impact parameter, $\hat{b} = 0.7$.

It is clear from the phase space of these simulations that when projectile and target are boosted towards each other, the target undergoes fragmentation and participant matter differs drastically.

The Fig 3.6 is showing the momentum space of the reaction $^{14}_{7}N + ^{86}_{36}Kr$. In case of asymmetric reaction due to unequal distribution of energy among the nucleons, the momentum distribution is also non-uniform.

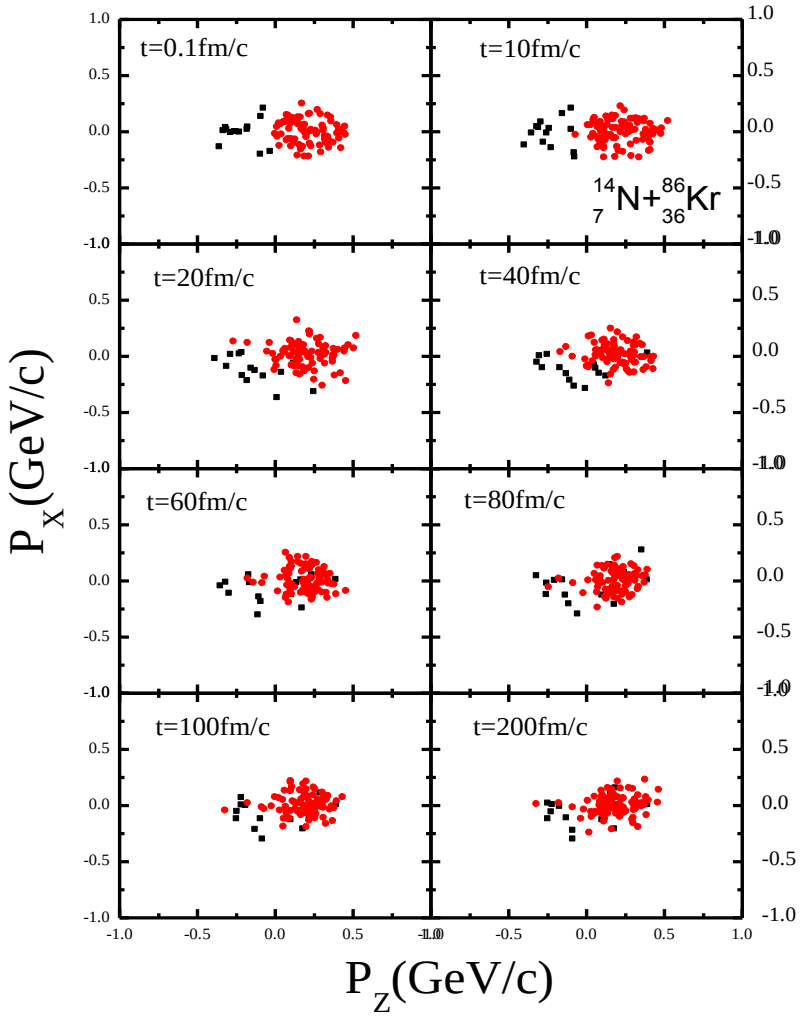

Fig 3.8: Momentum space of $^{14}_{7}N + ^{86}_{36}Kr$ at $E = 100MeV/nucleon$ and impact parameter, $\hat{b} = 0.7$.

3.5 Density Profile

After looking at the colliding phase of nuclear matter in coordinate and momentum space, the effect of the colliding nuclei on the local density of the combined nuclear matter can be seen.

The density of the i^{th} particle is given as

$$\rho_i(r) = \int f_i\big(r, p, r_i(t), p_i(t)\big) d^3p$$

$$= \frac{1}{(2\pi L)^{3/2}} e^{-[r-r_i(t)]^2/2L} \quad \text{.....(3.1)}$$

As, it is clear from the equation 3.1, the density of the nuclei will decrease exponentially with increase in the distance of the nucleon from the centre of the nucleus.

When the two asymmetric nuclei tend to collide with each other, their nucleons are unable to interact with each other due to the non-uniformity of the line connecting the centers of the two nuclei. As a result, due to less interaction, the normal nuclear matter density tends to decrease as compared to that in the case of symmetric nuclei. Fig 3.9 displays the density profile of reactions ${}^{45}_{19}K + {}^{55}_{25}Mn$ and ${}^{34}_{18}Ar + {}^{66}_{30}Zn$ at b=0 having $\eta = 0$ and $\eta = 0.3$ respectively using the liquid drop radius. The total mass of the systems is kept fixed in both the cases. The red line is showing the density variation of the target and the black line is showing the density variation of the projectile. At t=0.1fm/c, the combined density of the nuclear system is in close approximation with the normal nuclear matter density $\rho_0 \approx 0.16\text{fm}^{-3}$. As the time approaches to the next higher sage i.e at t=10fm/c, the local density of the system decreases. The effect of moving from a lower value of asymmetry to a higher value of asymmetry is clearly shown in the Fig 3.9. The density formed in the central region of projectile and target for $\eta = 0.3$ is slightly less than that of the case for $\eta = 0.1$.

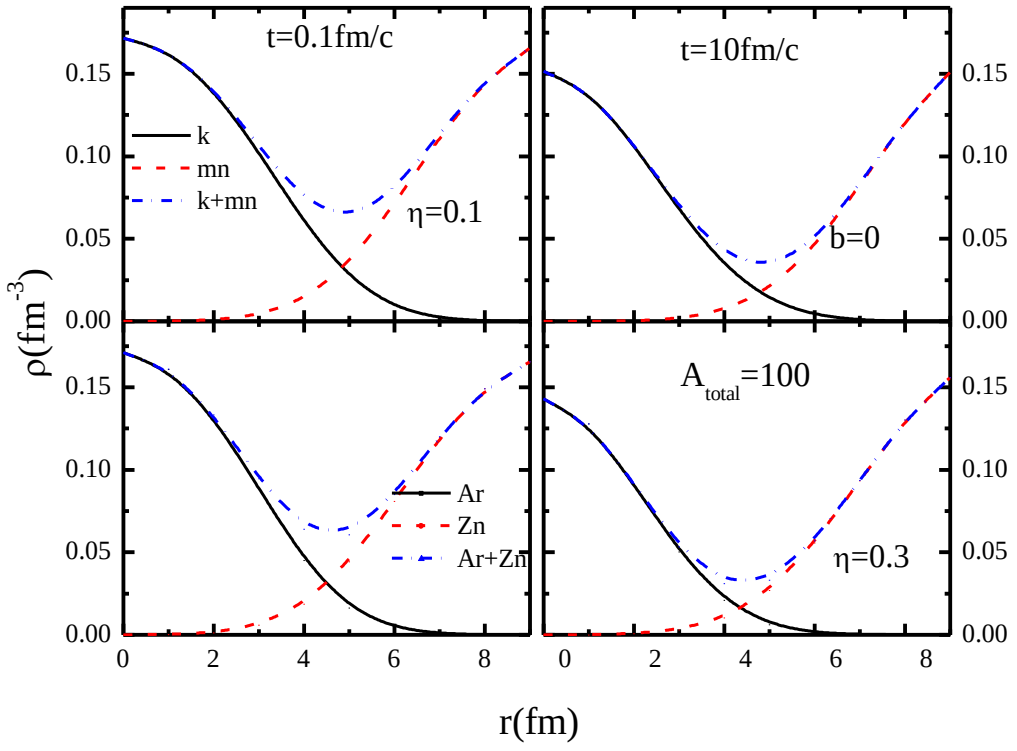

Fig 3.9: Time evolution of the local density for the reactions, ${}^{45}_{19}K + {}^{55}_{25}Mn$ and ${}^{34}_{18}Ar + {}^{66}_{30}Zn$ at b=0, having E=100MeV/nucleon.

The Fig 3.10 is showing the variation of local density with the reaction time for the same reactions as shown in the Fig 3.9 but at the larger value of impact parameter i.e. at $\hat{b}$ =0.5. As we have previously talked about that the rotational effect can be seen at higher impact parameters. The decrease in the density from $\rho = 0.150\text{fm}^{-3}$ to $\rho = 0.117\text{fm}^{-3}$ for ${}^{45}_{19}K + {}^{55}_{25}Mn$ and the decrease in the density from $\rho = 0.143\text{fm}^{-3}$ to $\rho = 0.099\text{fm}^{-3}$ for ${}^{34}_{18}Ar + {}^{66}_{30}Zn$ is pointing towards the less interacting nature of the nucleons of projectile and target due to which the projectile will tend to rotate around the target nuclei, since $A_T > A_P$. The percentage decrease in the value of density at t=10fm/c for $\eta = 0.1$ is 12% whereas for $\eta = 0.3$ is 18.18%. This

decrease of 6.18% is showing the significance of the higher mass asymmetry and that the rotational effect can be seen with a higher value of visibility at larger mass asymmetries.

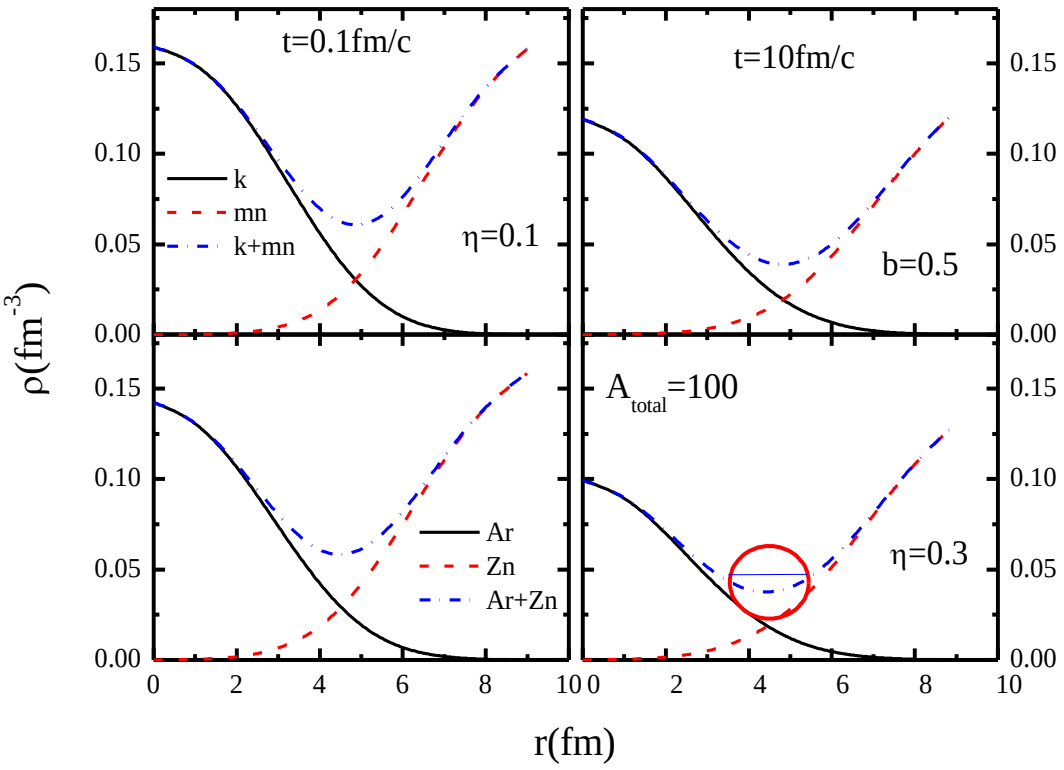

Fig 3.10: Time evolution of the local density for the reactions, ${}^{45}_{19}K + {}^{55}_{25}Mn$ and ${}^{34}_{18}Ar + {}^{66}_{30}Zn$ at b=0.5, having E=100MeV/nucleon.

The Fig 3.11 and Fig 3.12 are also showing the variation of local density with reaction time as shown in the Fig 3.9 and Fig 3.10 but the total mass of the colliding system is kept fixed at 248. In Fig 3.11, at $\hat{b}$ =0, the local density is increasing as we are moving from $\eta = 0.1$ to $\eta = 0.3$, which is in contrast with the first fig 3.9. This is due to the increase in the N/Z ratio as we move from $\eta = 0.1$ to $\eta = 0.3$ but the trend in the decrease in the density is same as that for the total mass 100 as we move from b=0 to b=0.5 but the percentile decrease in the density in this case is

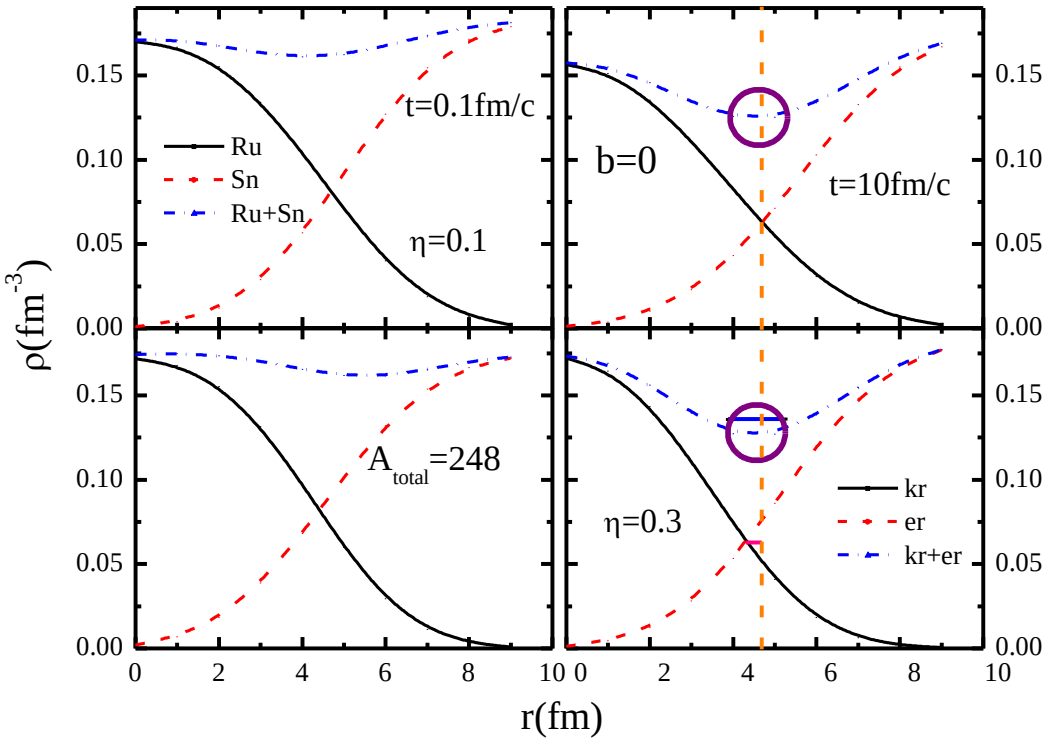

Fig 3.11: Time evolution of the local density for the reactions, ${}^{104}_{44}Ru + {}^{144}_{62}Sn$ and ${}^{86}_{36}Kr + {}^{162}_{68}Er$ at b=0, having E=100MeV/nucleon.

9.44%, almost an increase of 21% as we move from $A_{\text{Total}} = 100$ to $A_{\text{Total}} = 248$. This rise is due to the increase in the value of system's mass.

The variation of impact parameter can be clearly seen in the Fig 3.11 and Fig 3.12. The decrease in the local density of ${}^{104}_{44}Ru + {}^{144}_{62}Sn$ for (η=0.1) as we move from b=0 to b=0.5 is 0.008 i.e. a decrease of 2.61% and the change in density of ${}^{86}_{36}Kr + {}^{162}_{68}Er$ for (η=0.3) is 12.05%. A decrease of 12.04% is observed.

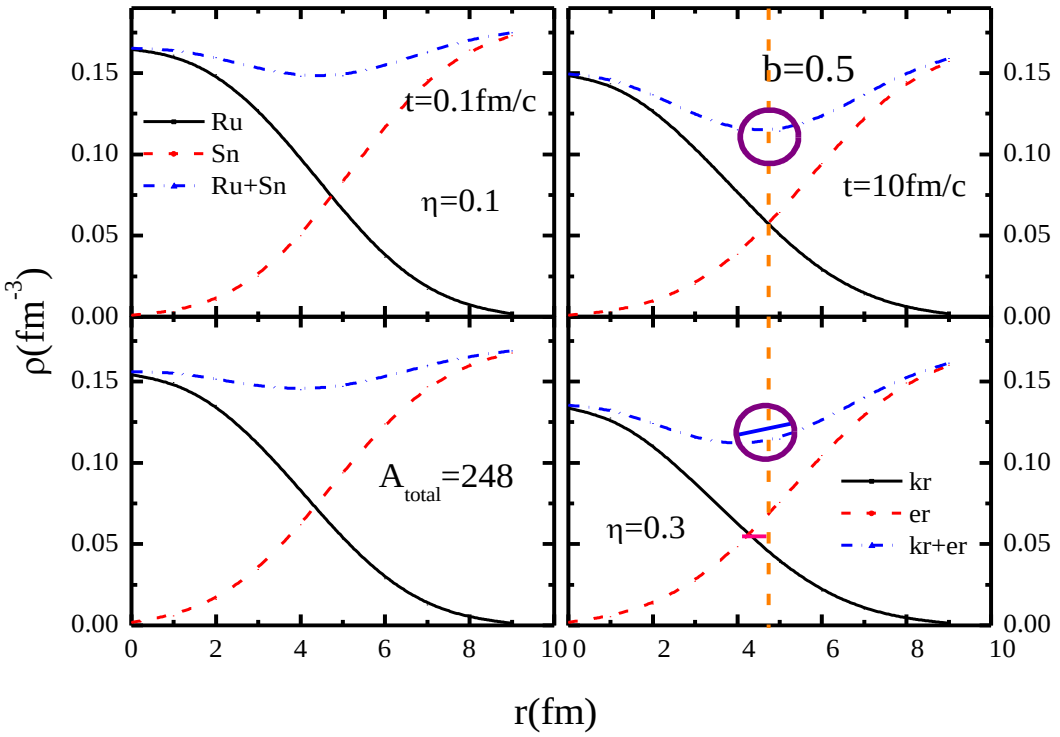

Fig 3.12: Time evolution of the local density for the reactions, ${}^{104}_{44}Ru + {}^{144}_{62}Sn$ and ${}^{86}_{36}Kr + {}^{162}_{68}Er$ at b=0.5, having E=100MeV/nucleon.

3.6 Study of temperature in heavy ion reactions

The variation of $< T_{avg} >^{max}$ with the scaled impact parameter $\hat{b}$ = b/b_{max} in Fig. 3.13 is seen. With the increase in the scaled impact parameter, the temperature of the central region reached in the heavy ion collisions for any mass asymmetry decreases. As the $\hat{b}$ is increased, a major difference in the temperatures for the different mass asymmetries is seen for the semi central collisions in comparison to the central and peripheral collisions. At η=0.7 and $\hat{b}$ =0.5, $< T_{avg} >^{max}$ decreases adruptly due to the increase in the mass asymmetry and decrease in the interaction region. Whereas, for central and peripheral geometry, the nucleon-nucleon collisions are uniform.

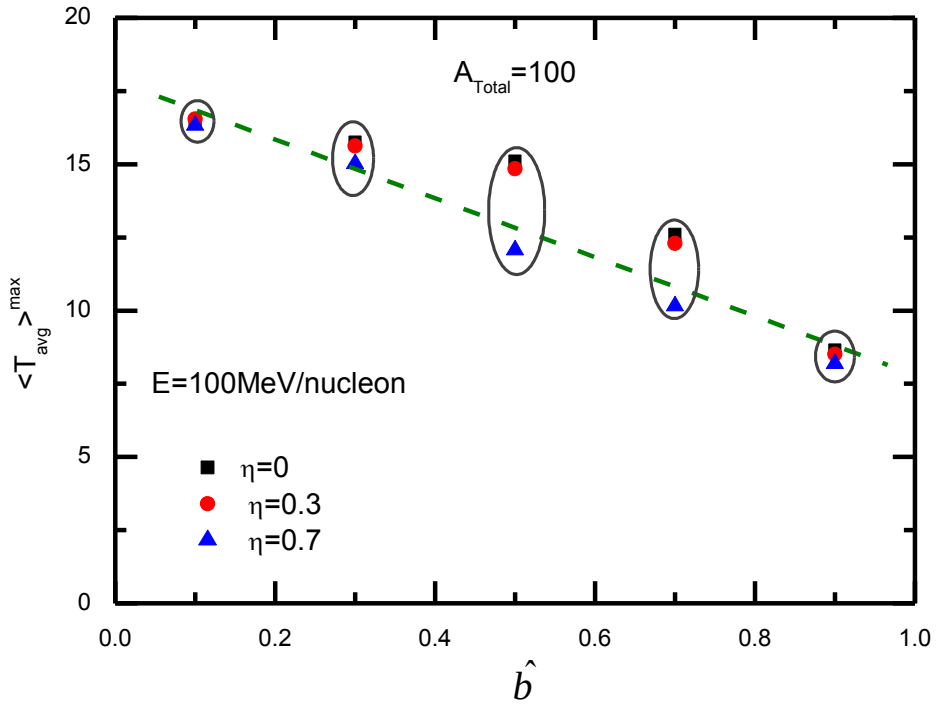

Fig 3.13: Variation of $< T_{avg} >^{max}$ with the scaled impact parameter.

As to see the temperature dependence on different mass asymmetric reactions, the effect of system's mass is being nullified by keeping the participant zone of the nuclei fixed to 50% of the total value of participant matter. 50% is an adequate value because at this value proper rotational effect of the two nuclei can be seen.

All the nucleons which have suffered at least one collision forms the participant matter and other nucleons are a part of spectator matter. The participant matter formed in the central collisions contributes a heavier amount to the combined nuclear matter formed in the reaction, whereas in the peripheral collisions the spectator matter provides a large part to the nuclear matter.

For the present analysis, the simulations are carried out for the following reactions. These simulations are carried out for both symmetric and asymmetric reactions.

Table 3.1: List of various nuclear reactions simulated under the framework of IQMD model

S.No.	Total Mass	Asymmetry Mass Parameter				
		η =0.0	η =0.1	η =0.3	η =0.5	η =0.7
1	100	$^{50}_{20}Ca + ^{50}_{20}Ca$	$^{45}_{19}K + ^{55}_{25}Mn$	$^{34}_{18}Ar + ^{66}_{30}Zn$	$^{25}_{12}Mg + ^{75}_{33}As$	$^{14}_{7}N + ^{86}_{36}Kr$
2	160	$^{80}_{36}Kr + ^{80}_{36}Kr$	$^{72}_{30}Zn + ^{88}_{40}Zr$	$^{54}_{26}Fe + ^{106}_{48}Cd$	$^{40}_{20}Ca + ^{120}_{52}Te$	$^{24}_{13}Al + ^{136}_{57}La$
3	200	$^{100}_{40}Zr + ^{100}_{40}Zr$	$^{90}_{36}Kr + ^{110}_{50}Sn$	$^{70}_{32}Ge + ^{130}_{52}Te$	$^{50}_{24}Cr + ^{150}_{66}Dy$	$^{30}_{14}Si + ^{170}_{70}Yb$
4	248	$^{124}_{50}Sn + ^{124}_{50}Sn$	$^{104}_{44}Ru + ^{144}_{62}Sn$	$^{86}_{36}Kr + ^{162}_{68}Er$	$^{62}_{28}Ni + ^{186}_{74}W$	$^{38}_{18}Ar + ^{210}_{82}Pb$

These reactions are carried out for different impact parameters ranging from $\hat{b}$ =0.1 to $\hat{b}$ =0.9. After fixing the participant zone to be fixed at 50%, a particular value of scaled impact impact parameter is chosen as shown in the Fig 3.14. The Fig 3.14 is showing the variation of participant matter with scaled impact parameter for total masses equivalent to 100, 160, 200, 248 for different mass asymmetries ranging from η=0.1 to η=0.7. The participant matter decreases as the value of scaled impact parameter is increased, since increased value of scaled impact parameter give rises to the peripheral collisions. The variation for the participant matter (P.M) is as

$$(\mathrm{P.M})_{\eta=0} > (\mathrm{P.M})_{\eta=0.1} > (\mathrm{P.M})_{\eta=0.3} > (\mathrm{P.M})_{\eta=0.5} > (\mathrm{P.M})_{\eta=0.7}$$

The percentage (%) change in the value of participant matter on going from η=0.1 to η=0.7 for the two extreme values of scaled parameter is shown in the table.

As can be seen from the table, the difference in the % change between the two different impact parameters is small for the same system mass. Whereas the difference in the % change between

the two different masses is small for the same impact parameter. The percentile increase in the value of participant matter for the variation from $\hat{b}$ =0.1 to $\hat{b}$ =0.9 for the same mass is negligible but the percentile increase in the value of participant matter for different mass is large enough to notice. This is due to increased number of nucleons taking part in the formation of participant matter with increase in the mass of the system.

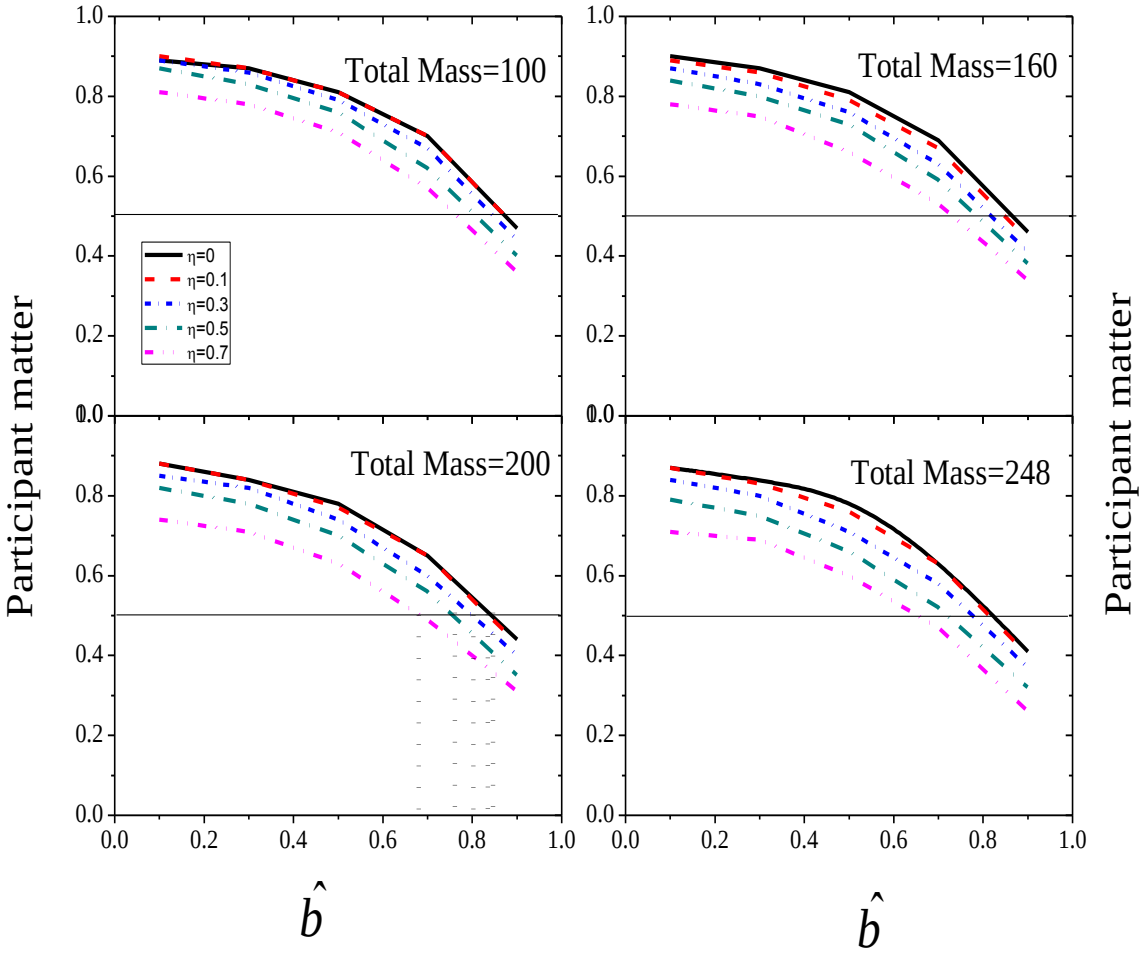

Fig 3.14: Time evolution of participant matter for systems having different mass.

After a 50% cut on participant matter, the following table has been constructed.

Table 3.2: List of fixed values of $\hat{b}$ (Impact Parameter) at which the simulations have to be carried out according to the reactions as given in the table 3.1.

S.No.	**Total Mass**	$\hat{b}$ **(Impact Parameter)**				
		n=0	n=0.1	n=0.3	n=0.5	n=0.7
1	100	0.877	0.871	0.849	0.811	0.767
2	160	0.864	0.845	0.818	0.786	0.731
3	200	0.816	0.835	0.779	0.758	0.666
4	248	0.822	0.610	0.777	0.719	0.672

According to these constrained values of $\hat{b}$, the simulations are carried out for the same reactions as shown in the table1. The simulations are carried out for $E_{Lab} = 100 MeV/nucleon$. This value of energy has been taken due to the fact that at this value both the mean field interaction between the nucleons and nucleon - nucleon collisions plays a simultaneous part. So, in order to study the mass asymmetric effects on the temperature, the effect of both system's mass and geometry of the reaction is nullified.

Since, the present analysis deals with the temperature extraction, the variation of average density ($< \rho^{avg}/\rho_0 >$) and maximum density ($< \rho^{max}/\rho_0 >$) with reaction time is seen.

The density discussed here is the global density. The density can be calculated as

$$\rho(r,t) = \sum_{i=1}^{A_T+A_P} \frac{1}{(2\pi L)^{\frac{3}{2}}} . \exp\left[-\left(r - r_i(t)\right)^2/2L\right]$$

L is the Gaussian width of the wave packet. A_P and A_T are the masses of projectile and target respectively. The density is calculated in the central sphere of radius of 2fm. This formulation of density gives the two possibilities of looking into the average value and maximum value of density. This can be seen from the variation of $< \rho_{max}/\rho_0 >$ and $< \rho_{avg}/\rho_0 >$ with reaction time for the symmetric reaction ${}^{197}_{79}Au + {}^{197}_{79}Au$ at the energy $E = 100MeV/nucleon$ and at $\hat{b}$ =0. As we know that maximum temperature will reach when nuclear matter is highly compressed. Therefore, we have carried out the calculation of temperature at the maximum value of $< \rho_{max}/\rho_0 >$ and $< \rho_{avg}/\rho_0 >$.

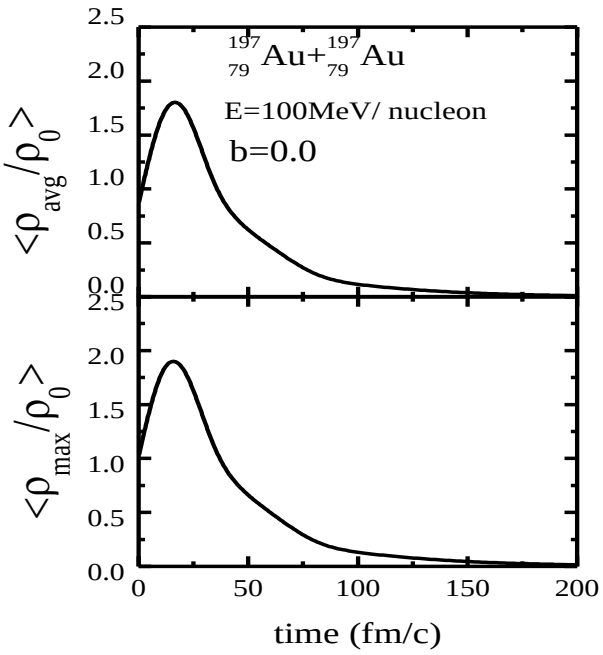

Fig 3.15: Time evolution of $< \rho^{avg}/\rho_0 >$ and $< \rho^{max}/\rho_0 >$ for the reaction, $^{197}_{79}Au + ^{197}_{79}Au$, at $E = 100MeV/\,nucleon$.

The local temperature can be calculated using hot Thomas Fermi approach as discussed in the previous chapter.

The model used for the calculations is IQMD model as discussed in the previous chapter. The fig is showing the variation of $< \rho^{avg}/\rho_0 >$ and $< T^{avg} >$, with reaction time for different A_{Total}. At the start of the reaction, the temperature of the central part begins to increase, reaches at the maximum value, and then it starts decreasing because now the matter starts expanding approximately after t=20fm/c. The same trend is seen for the density. In contrast to density, the temperature variation is showing fluctuations. This is due to the fact, that the random collisions of the nucleons in the fireball raise the temperature of the nuclear matter.

In fig 3.16 and fig. 3.17, the value of maximum value of $< \rho^{avg}/\rho_0 >$ and $< T^{avg} >$ with higher mass asymmetry (η) increases. The maximum value of $< T^{avg} >$ reaches faster (around 20fm/c) for η=0.7, while for η=0, it is about 30fm/c, although the total mass of the system is same for both the asymmetries. This time delay in the maximum value is due to the energy

distribution due to nucleon-nucleon collisions. In case of higher asymmetry, the energy distribution is non-uniform and this non-uniform distribution raises the density and temperature of the central region earlier. In case of symmetric nuclei, the distribution is uniform. It is concluded from the fig. 3.16 and fig. 3.17 that the maximum value of $< T^{max} >$ is higher than the value of $< T^{avg} >$.

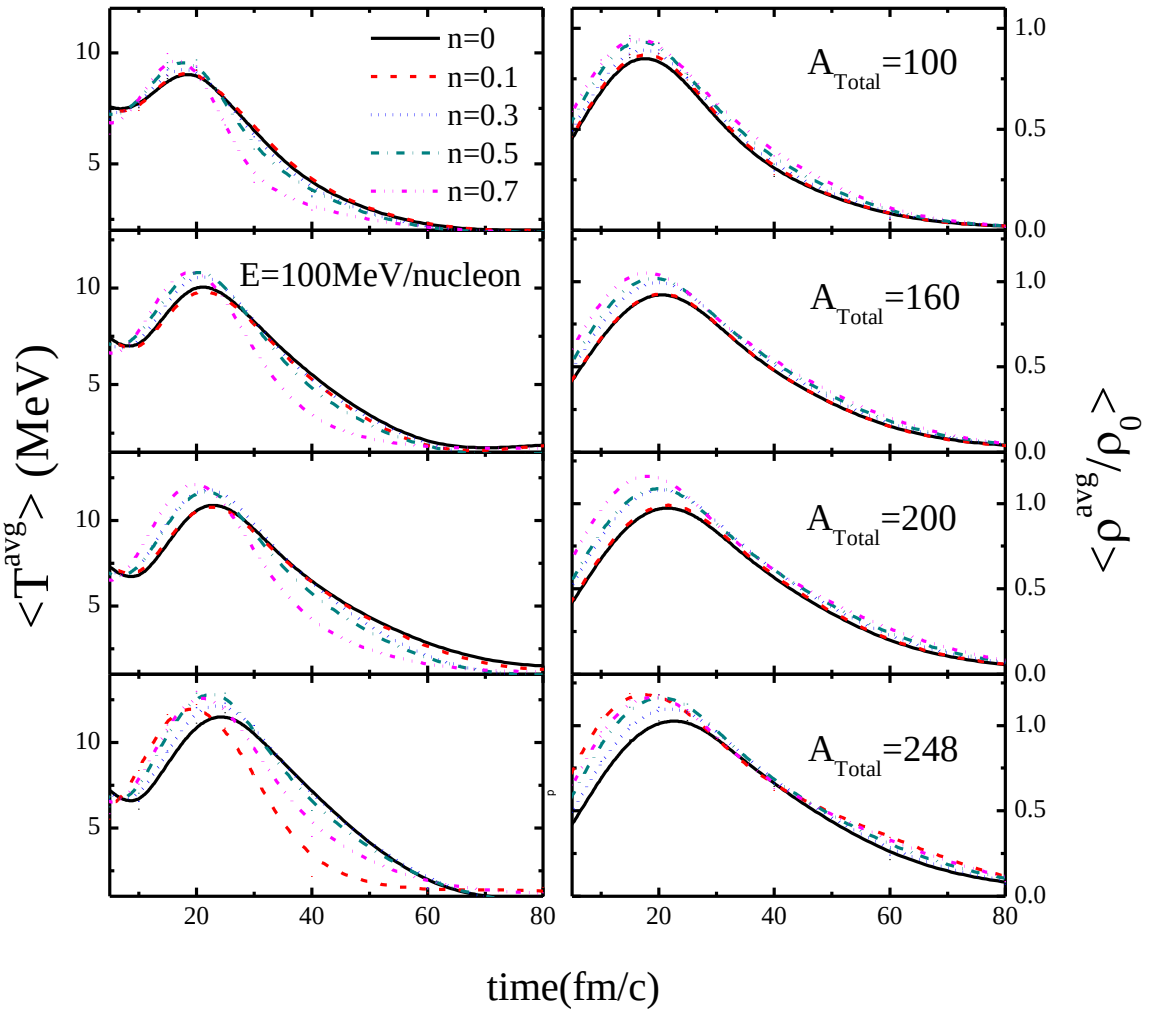

Fig 3.16: Time evolution of $< \rho^{avg}/\rho_0 >, < T^{avg} >$, at $E = 100MeV/\,nucleon$ at different mass asymmetries for different A_{Total}.

Because, $< T^{avg} >$ is the temperature averaged over all the nucleon collisions at a particular reaction time. And $< T^{max} >$ is the maximum temperature reached out of the many collisions. The value of $< \rho^{avg}/\rho_0 >$ and $< \rho^{max}/\rho_0 >$ is almost similar for the heavier systems. This is due to the formation of uniform dense matter and for the lighter systems, no such similarity is observed. This is due to the formation of non-uniform distribution due to the system's mass. Also, it is clear that the density profile for higher mass asymmetry resembles the density profile for the lighter mass nuclei and that for symmetric and nearly symmetric matches with the heavier ion.

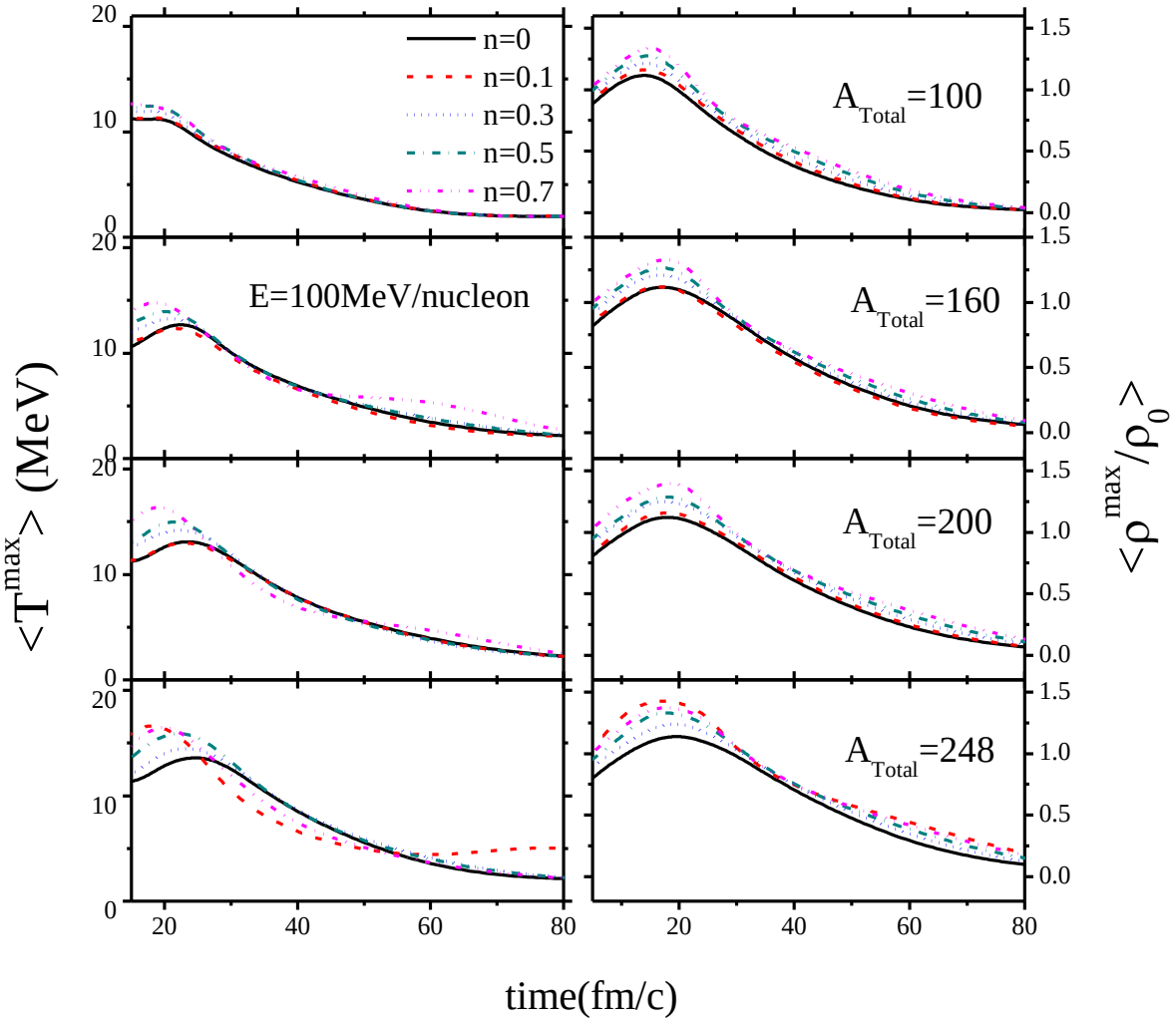

Fig 3.17: Time evolution of $< \rho^{max}/\rho_0 >, < T^{max} >$, at $E = 100MeV/\,nucleon$ at different mass asymmetries for different A_{Total}.

After this the variation of $< \rho^{avg}/\rho_0 >_{Max}$, $< \rho^{max}/\rho_0 >_{Max}$, $< T^{avg} >_{Max}$, $< T^{max} >_{Max}$,with the total mass of the system is displayed. As, it can be clearly seen, that, if we nullify the system's mass effect, as well as geometry of the system, even then the complete equilibrium is not reaching. As we have fixed the participant zone, the temperature for the different mass asymmetries should come out to be same. But this is not the case. A scattered pattern is observed rather than a uniform pattern.

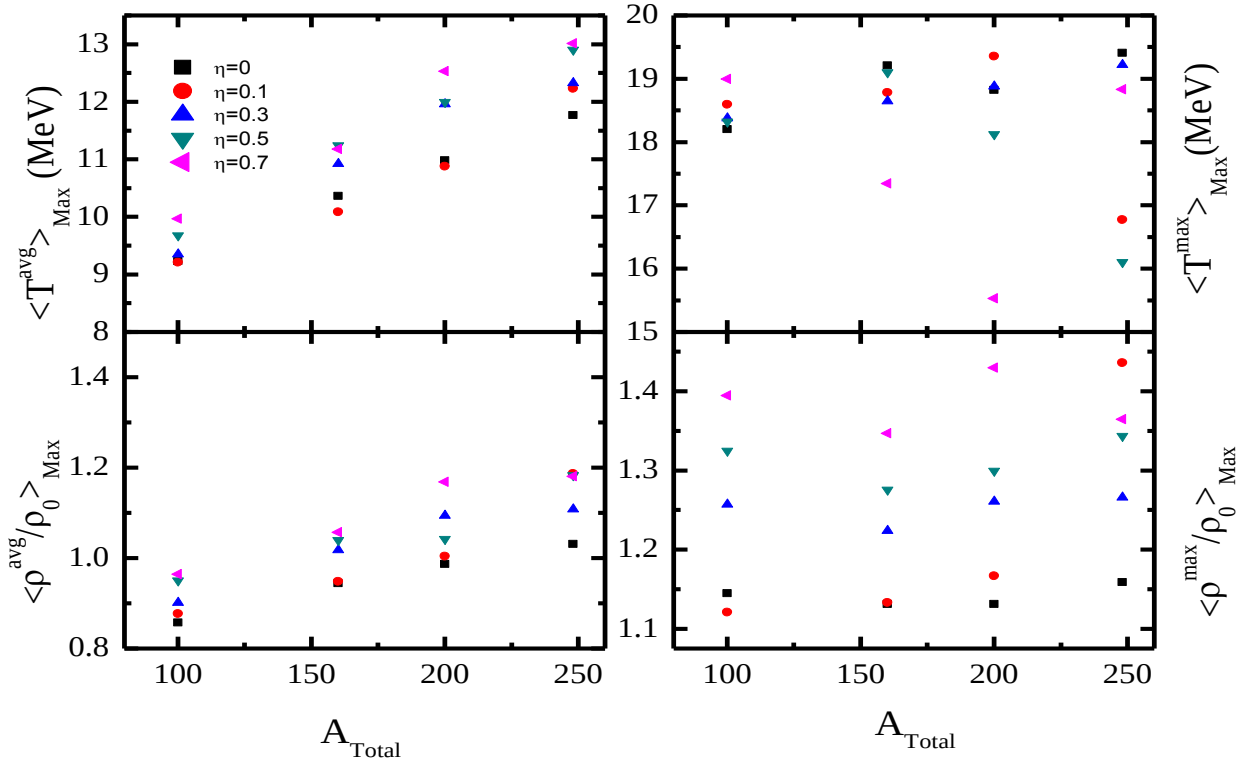

Fig 3.18: The variation of with$< \rho^{avg}/\rho_0 >, < \rho^{max}/\rho_0 >, < T^{avg} >, < T^{max} >$with Atotal.

This scattering is due to the rotational effect. As we move towards the higher asymmetry, the influence of rotational effect also increases or we can say that the number of rotations that a projectile undergoes around the target is not same for different mass asymmetries.

Whenever, asymmetric nuclei collide with each other, it can result in enhanced number of rotations of the lighter nuclei around the heavier one. The number of rotations increases as one move towards the higher mass asymmetry. The irregularity observed in the variation of $< T^{avg} >_{Max}$ is also due to this effect. Also, this effect can be due to the nucleons present in the core, which are making a transition from core to surface or vice versa, as can be seen from Fig. 3.18.

SUMMARY

In the present study following results have been concluded.

- As the $\hat{b}$ is increased, a major difference in the temperatures for the different mass asymmetries is seen for the semi central collisions in comparison to the central and peripheral collisions.

- With increase in the system's mass, the temperature increases due to the increased number of nucleons.

- It has been revealed that the temperature of the hot dense central region formed in HIC's is not same even if the nucleons in the same volume for different mass asymmetric reactions. This is due to the rotation effect created in the asymmetric systems. Due to this rotational effect, the energy of the whole system is increased, due to which complete equilibration for the different mass asymmetric nuclei is not reached. Another reason of these fluctuations can be the transitions of nucleons from the surface and core of the nucleus or vice versa.

REFERENCES

[1] R.A. Alpher and R.C. Herman, "Remarks on the evolution of the expanding universe", Phys. Rev. **75** , 1089, (1949).

[2] International Review Of Nuclear Physics vol 6, (1991), edited by László P. Csernai, D. Strottman.

[3] G.Chaudhuri, S. Maliik and S. Das Gupta, Journal Of Physics, **420**, 012098, (2013).

[4] O. N. Ghodsi and R. Gharaei, Phys. Rev. C **84**, 024612 (2011).

[5] T. Gaitanos, H. H. Wolter and C. Fuchs, Phys. Lett. B 478, 79-85, (2000).

[6] P. J. Siemens, J. O. Rasmussen, Phys. Rev. Lett., **42** (1979) 880.

[7] T. Gaitanos et. al, proceedings of the XXXVIII International Winter Meeting on Nuclear Physics, Bormio, Italy, January, 2000.

[8] T. Odeh, et al., Phys. Rev. Lett (2000).

[9] M. Lisa and the EOS collaboration, Phys. Rev. Lett. **75** (1995) 2662.

[10] W. Reisdorf and the FOPI Collaboration, Nucl. Phys. A **612** (1997) 493.

[11] A. Hombach, W. Cassing, S. Teis, U. Mosel, Eur. Phys. J. A 5 (1999) 157.

[12] Y. Hama, T. Kodama and O. Socolowski Jr, Brazilian Journal of Physics, vol. 35, no. 1, (2005).

[13] D. T. Khoa et. al, Nucl. Phys. A **542,** 671-698, (1992).

[14] D. T. Khoa et. al, Nucl. Phys. A**583,** 353-356, (1995).

[15] D. T. Khoa et al., Nucl. Phys. A **548**, 102 (1992); R. K. Puri et al., ibid. **575**, 733 (1994).

[16] J. Liu, W. Guo, S. Wang, W. Zuo, Q. Zhao and Y. Yang, Phys. Rev. Lett. **86**, 975 (2001).

[17] S. Gautam, Phys. Rev. C **83**, 064604 (2011).

[18] K.Vinayak et. al, Eur. Phys. J A **48** 96 (2012).

[19] S. Goyal, Physics Research International, pp 1-10, Volume 2014, 2014.

[20] A. D. Sood and R. K. Puri, "Nuclear dynamics at the balance energy," Physical Review C,vol. 70, Article ID 034611, 2004.

[21] H. Kruse, B. V. Jacak, and H. Stocker. Phys. Rev. Lett. 54, 289 (1985).

[22] J. J Molitoris and H. Stocker, Phys. Rev C 32, R346 (1985).

[23] C. Hartnack, R. K. Puri, J. Aichelin, J. Konopka, S. A. Bass, H. Stocker, and W. Greiner, Eur. Phys. J. A 1, 151 (1998).

[24] C. Hartnack and J. Aichelin, J. Phys. G: Nucl. and Part. Phys. 28, 1649 (2002);

ibid. 30, 531 (2004).

[25] F. Daffin, K. Haglin, W. Bauer Phys. Rev. C 54, 1375, (1996).

[26] C. Hartnack et al., Nucl. Phys. A 495, 303 (1989)

[27] J. Aichelin, Phys. Rep. **202**, 233 (1991).

[28] L. Neise, et. al, Nucl. Phys **A 519**, 375 C (1990).

[29] A. Bohnet, Ph.D Thesis, University of Heidelberg (1988).

[30] S. A. Bass, C. Hartnack, H. Stocker, and W. Greiner, Phys. Rev. C 51, 3343 (1995);

B. J. VerWest and R. A. Arndt, Phys. Rev. C **25**, 1979 (1982)

[31] P. Danielewicz and G. F. Bertsch, Nucl. Phys. A 533, 712 (1991).

[32] K. Chen, et. al, Phys. Rev. **166**, 949 (1968).

[33] R. R. Betts, in Proceedings for the Conference on Resonances in Heavy Ion Reactions, edited by K. A. Eberhardt, Lecture Notes in Physics Vol. 156, p. 185, (Springer, Berlin, 1981).

[34] Varinderjit Kaur and Suneel Kumar, Phys. Rev. C **81**, 064610 (2010).

[35] S. Goyal, International Symposium on Quasifission Process in Heavy Ion Reactions, Journal of Physics: Conference Series 282, 012023 (2011).

[36] D. Kaur et. al, Ukr. J. Phys. Vol. 57, No. 8, (2012).

[37] S. Gautam, Eur. Phys. J. A, **48** : 3, (2012)